TÉCNICO LISBOA

Optimization of Gateway Deployment in Smart Metering LoRaWAN Networks

Madalena Maria Muller e Sousa Avillez Albuquerque

Thesis to obtain the Master of Science Degree in

Electrical and Computer Engineering

Supervisor: Prof. António Manuel Raminhos Cordeiro Grilo

Examination Committee

Chairperson: Prof. Teresa Maria Sá Ferreira Vazão Vasques
Supervisor: Prof. António Manuel Raminhos Cordeiro Grilo
Member of the Committee: Prof. António Luís Campos da Silva Topa

March 2021

Declaration

I declare that this document is an original work of my own authorship and that it fulfills all the requirements of the Code of Conduct and Good Practices of the Universidade de Lisboa.

To my parents

Acknowledgments

First of all, I want to thank my supervisor, Prof. António Manuel Raminhos Cordeiro Grilo, for the unconditional guidance, for the constant availability and will to teach. I feel privileged for all the knowledge I earned from working with Prof. António Grilo.
To my parents, Inês and Duarte, my brothers, Sebastião and Salvador for the unconditional support and believe, and for always being there for me in the good and bad times throughout my life.
To my friends, I want to show my gratitude for their loyalty, for standing by me no matter what, and for all the unforgettable moments we had along the years.

Resumo

Recentemente, as redes de longa distância e de baixa potência (*Low Power Wide Area Network-LPWANs*) atraíram um grande interesse devido à necessidade de conectar cada vez mais dispositivos à chamada Internet das Coisas, (*Internet of Things - IoT*). Observou-se o desenvolvimento da tecnologia *Long Range* (LoRa) como uma tecnologia emergente adequada para redes inteligentes (Smart Grids - SG). Sendo assim, este trabalho usa considerações teóricas para desenvolver um modelo de canal de LoRa que considera a atenuação em espaço livre, efeito de *shadowing* e efeito *fading*.

Neste contexto, esta dissertação de mestrado propõe um modelo teórico para estimar as posições ótimas das *gateways* de LoRa. Cada simulação considera *smart meters* com localizações fixas e posteriormente calcula curvas de Pareto com o algoritmo de otimização NSGA-II, com ambos os objetivos: minimizar o número de *gateways* combinado com a menor perda de pacotes do canal. A perda de pacotes e a distância entre os nós são estimadas teoricamente.

Os resultados mostram uma diminuição significativa da interferência do sinal, na presença de *fading* ou *shadowing*. Este comportamento teve um efeito considerável na otimização da rede e estudou-se a possibilidade do efeito de *fading* e *shadowing* poder causar a diminuição da perda de pacotes devido à ortogonalidade do *spreading factor*.

A contribuição deste trabalho é o estudo do impacto dos fenómenos de *fading* e *shadowing* na otimização e desempenho de redes LoRaWAN.

Palavras-chave: LoRa, Gateways, Fading, Shadowing, NSGA-II, LoRaWAN

Abstract

Recently, Low Power Wide Area Networks (LPWANs) have attracted great interest due to the need of connecting more and more devices to the so-called Internet of Things (IoT). We have witnessed the development of Long Range (LoRa) technology as an emerging technology suitable for smart grids (SG). Therefore, this work uses theoretical considerations to develop a channel model of LoRa that considers propagation attenuation, shadowing, and fading effect.

Hence, a theoretical model developed in this study proposes to estimate the optimal gateways positions of LoRa. Each experiment considers smart meters with defined locations and plots the NSGA-II Pareto optimal curve with both objectives: the minimum number of gateways combined with the packet loss of the channel. The packet loss and distance between nodes are estimated theoretically.

Results show a significant decrease in the signal interference in the presence of fading or shadowing. This effect had a considerable impact on the network's optimization. Therefore, this led the study to find that the effect of fading and shadowing can reduce packet loss because of the spreading factor's orthogonality. The contribution of this work is the study of the impact of fading and shadowing on the optimization of LoRaWAN network's deployment.

Keywords: LoRa, Gateways, Fading, Shadowing, NSGA-II, LoRaWAN

Contents

List of Tables

List of Figures

Chapter 1

Introduction

1.1 Motivation

Traditional networks weren't developed for a typical Internet of Things (IoT) scenario. The power consumption from the connected network devices is too high and so is the cost of its connectivity when the number of devices in the network scales. More recently Long Power Wide Area Network (LPWAN) technologies were developed to meet the requirements of the IoT, being able to cover huge numbers of low power devices, allowing device lifetimes in the order of years.

Long Range Wide Area Network (LoRaWAN) is such a LPWAN technology whose presence is increasing. This technology is popular in battery-powered systems that require transferring a small amount of data at short intervals over long range. A LoRaWAN network capacity depends on many factors such as the distance between the end-nodes. There must exist a trade-off between coverage and costs and ideally, all devices have a gateway (GW) close by. This increases the performance and decreases the consumption of the devices, increasing their lifetime. However, as the number of devices scale, better coverage requires more GWs, which increases the costs of network's installation and maintenance. To optimize this problem, the distance from every end-device to the GW should be minimum without exceeding a large number of GWs. Optimizing this distance, the overall consumption decreases and the global network performance improves, reducing the economic cost. This thesis aims to analyze the impact of fading and shadowing phenomena in the trade-off between coverage and cost. Hence, the results will optimize the limited number of GWs locations and maximize the signal performance for a fixed number of smart meters. For this accomplishment, a LoRaWAN analytical model and implementation of an optimization algorithm to determine the best GW's positions are developed for different propagation models.

1.2 Topic Overview

Nowadays, electricity is essential as it powers most of the everyday life devices as well as commercial buildings, industries, the Internet, etc. Therefore, modern society's demand for electric power is increasing

as the delays and outages have a significant negative impact on their quality of life.

To overcome this dependence, Smart Metering (SM) through smart meters and smart grids is a strong solution to reduce the power supply-demand and increase its reliability. Smart meters expect to transmit their data using network technology and LPWAN is a promising technology, such as PLC and 4G/5G.

The performance of LPWANs, where LoRa networks are included, has spurred much interest in recent times due to the high interest in connecting more and more devices to the IoT. The massive number of connected devices associated to its random spatial deployment and random network access introduce new degrees of freedom, demanding for innovative performance evaluation approaches.

LoRaWAN is one of the most deployed LPWAN technology, gaining greater interest from the research and industrial communities. From theoretical aspects, many studies have focused on the performance and characteristics of LoRaWAN communications. The key parameters to optimize network performance for a realistic deployment is to correctly predict the coverage. Therefore, precise modeling of radio propagation characteristics and GWs positions is very crucial for LoRaWAN network planning and optimization. Radio propagation characteristics have been widely studied over the world. Numerous field measurements have been carried out in various indoor and outdoor environments in the context of cellular and wireless sensor networks. Generally, the path-loss is impacted by many factors such as distance, frequency band, average antenna heights, geography, and terrain in terms of obstacles, buildings, hills, mountains, people, etc. Furthermore, studies show that fading and shadowing can have a significant influence on network performance.

As it is well-known a transmitted signal has modifications while traveling through the propagation path to the receiver. The effect of these changes is commonly called fading. In free-space, a signal follows one path and arrives at the receiver with little attenuation. This is not the case for a signal that encounters obstacles in the propagation path. Instead, the signal is reflected, diffracted, and scattered from objects that are present in the path. Path loss, shadowing effect, and Rayleigh fading are the principal factors used to calculate the signal power in the receiver. Researchers are actively making efforts towards a future, where devices can be seamlessly integrated into a network and provide universal computing. LoRa is one of the most prominent technologies for long-range connectivity in IoT systems. As such, this work tries to find optimal GW locations maintaining a quality-signal performance.

1.3 Objectives

The objective of this Master thesis study is to evaluate the impact of fading and shadowing phenomena in the optimization of the LoRaWAN GWs deployment. For this accomplishment, a theoretical model of Lora was implemented considering the effects of fading and shadowing in signal propagation. For the optimized locations, this study developed a NSGA-II algorithm in order to optimize the quality signal with the lowest number of GWs possible, leading to a reduction of the cost.

1.4 Thesis Outline

The remainder of this document is structured as follows. Chapter 2 reviews the most important aspects of LPWANS, emphasizing some solutions that have a strong impact on wireless communications. LoRaWAN network and protocol are explained with all its specifications and regulations. Also in the same chapter a detailed explanation of NSGA-II, a Multiobjective optimization algorithm, is provided. In Chapter 3, a preview of the LoRaWAN analytical model developed by INESC in WimecoM is given. The first contributions of this thesis are proposed with the study of fading and shadowing in the quality performance of the network. Chapter 5 contains the simulation results of the network performance that was developed. Four scenarios were considered and compared: an ideal scenario with log-distance propagation model and three more realistic scenarios affected by shadowing and Rayleigh fading. Finally, Chapter 6 presents the final conclusions, achievements and future work of this Master thesis.

Chapter 2

State of Art

This chapter serves as an overview on the background of this thesis study components. A general explanation of the smart meters and SGs importance in our days is given. A brief description of LoRa and comparison to other LPWAN technologies is provided. Then, this chapter presents all parameters and specifications of the network LoRaWAN. Also in this Chapter, the NSGA-II algorithm is described in detail among with it's operations and theoretical definitions. To conclude, some studies related to this thesis are discussed and their contributions and positive conclusions are highlighted.

2.1 Smart Metering Infrastructure

Smart meters are powerful measurement devices that have a digital display, capabilities of recording how much power is consumed, and transmitting this information automatically. With a smart meter, electrical data such as voltage and frequency are measured and real-time energy consumption information is registered. These devices support bidirectional communication between the meter and the central system. A smart meter is one of the most important devices used in the SGs.

A SG is an electrical network based on digital technology that is used to supply energy to consumers. This system allows for monitoring, analysis, control, and communication within the supply chain to help improve efficiency, reduce energy consumption and cost, and maximize the transparency and reliability of the energy supply network.

The SG was introduced to overcome the weaknesses of conventional electrical grids. There are several telecommunication technologies utilised by SM applications and they are mainly distinguished according to the transmission medium used for the signals.

2.1.1 Technologies for Smart Grids

In this section, a brief description of some technologies used for SG deployment is presented. Despite the existence of many technologies that could be analyzed and discussed, the most relevant to refer according to this thesis research are PLC, Zigbee, and 5G mMTC.

One basic type of smart meter system communication technology is Power Line Communications (PLC). PLC carries data on a conductor that is also used simultaneously for electric power transmission or electric power distribution to consumers. This data can then be used for operational purposes and predict the future benefits of a business. Therefore, this technology can improve cost-effectiveness for rural lines and make it possible to work for remote areas or over long distances. As Advanced Metering Infrastructure (AMI) continues to gain traction (especially in new or developing markets), the choice of potential communication technologies also continues to expand. PLC still dominates the communicating meter market overall but the emerging trend suggests a move towards new technologies for some utilities. Even if some of the most exciting opportunities exist in distribution grid applications (such as distribution automation), there is an opportunity within SM too.

ZigBee Smart Energy (SE) is a standard for interconnecting and interoperating devices, via radio frequency, directed towards monitoring, managing and automating energy, gas and water usage. It seeks to be a useful tool for creating “Green Homes”, and is aimed at coordinating energy usage, optimizing its generation and consumption. ZigBee is a simple data transmission protocol designed to be used as a low rate wireless personal area network (LR-WPAN). Based on the IEEE 802.15.4 specification, for a set of high-level communications protocols, it’s a low-powered, low-bandwidth digital radio communication system. Among its most important applications are automation in the home and SM. All in all, Zigbee has shown to have limited range and capacity.

5G is the fifth generation technology standard for cellular networks, which cellular phone companies began deploying worldwide in 2019. 5G wireless technology is meant to deliver higher multi-Gbps peak data speeds, ultra low latency, more reliability, massive network capacity, increased availability, and a more uniform user experience to more users. Higher performance and improved efficiency empower new user experiences and connects new industries. Massive Machine-Type Communications (mMTC) would be used to connect to a large number of devices. Although 5G mMTC seems very suitable for SM, there are still diverse challenges to overcome. [1].

Apart from solutions described above, there are emerging technologies that would be suitable for the realization of the IoT. Such technologies are suitable for SM and will be discussed in the next section.

2.2 LPWAN Technologies

Low power wide area network (LPWAN) is a type of wireless communication designed for sending small data packages over long distances at a low bit rate. LPWANs are fundamental for the IoT since these networks provide long-range coverage to end nodes, exploiting license-free frequency bands. There are free frequencies for anyone to use such as 863-870 MHz for Europe, free frequencies reserved for a specific application, and frequencies that can be bought from the country regulator such as some used in mobile phone systems.

Several LPWAN technologies have been developed in the last years making use of Radio Frequency modulation techniques and occupy parts of the RF spectrum that were only recently been designated

available for data communication. Some of these technologies are open source and can be used without licensing, such as Narrowband IoT (NB-IoT). On the other hand, there are other proprietary technologies that require a license to be used such as SigFox.

2.2.1 SigFox

Sigfox is a French company with a proprietary protocol that provides communication service. This LPWAN technology has shown a lot of potential and its reach has been steadily expanding. Sigfox is an Ultra Narrow Band technology indicated for lightweight use cases and characterized for using D-BPSK modulation. This bidirectional communication network uses the 868MHz band (Europe) with an uplink limit of 140 messages per day and 12 bytes per message. On the other hand, the implementation of downlink communication has a maximum of 8 bytes per message and 4 messages a day. Each message is 100 Hz wide, providing a maximum bit rate of 100 bit per second. The long-range is accomplished as a result of very long and very slow messages.

2.2.2 NB-IoT

NB-IoT is also a radio technology standard specified by the 3rd Generation Partnership Project (3GPP). The standards organization developed several protocols for mobile communications offering LPWA (Low Power Wide Area) technologies as solutions for the IoT demands.

NB-IoT reuses some of the LTE technical components but limits the bandwidth to 200kHz. By using a narrow-band reduces power consumption. This technology connects to an operator network through a licensed spectrum with a maximum bandwidth of 200 Hz and 200kps data rate. Like Sigfox and LoRa it provides bidirectional communication with unlimited messages with maximum payload of 1600 bytes. Furthermore, NB-IoT coexists with LTE and 2G/3G/4G.

2.2.3 Comparison between LPWAN technologies

LoRaWAN data rate is not the highest among its competitors, however, the type of applications that use LoRaWAN do not require high data rates. Its batteries last longer than other technologies, it saves more power, and it is more immune against interferences. The following Table 2.1 compares some features between LoRa, Sigfox and NB-IoT:

By examining the table, we can conclude its main competitor is NB-IoT. Comparing them, LoRaWAN is focused on lower-cost, high-volume applications, whereas NB-IoT is focused on high-value applications and quality of service. Also, LoRa devices have longer battery life than NB-IoT devices.

Some other competitors are: Ingenu and Weightless. Ingenu uses the 2.4 GHz band, and its main feature is its high data rate up to 624 kbps for uplink and 156 kbps for downlink; however, its range extends up to 6 kilometres, and it consumes more energy because of the band used. The Weightless Special Interest Group has developed three standards: Weightless-W, Weightless-N and Weightless-P. Weightless-W uses the whitespaces left by television (470 – 790 MHz), its data rates go from 1 kbps to

Table 2.1: Comparison between LPWAN technologies [2] [3]

	LoRaWAN	**Sigfox**	**NB-IoT**
Modulation	SS Chirp	UNB/GFSK/DBPSK	UNB/GFSK/BPSK
Bandwidth	125 – 500 kHz	100 Hz	100 Hz
Data Rate	290bps - 50Kbps	100-600 bps	100pbs
max nº mess/day	Unlimited	Limited	Unlimited
Link budget	154 dB	146 dB	151 dB
Battery Lfetime	8-10 years	7-8 years	1-2 years
Security	Yes	Yes	No
Range	5km (urban),	10km (urban)	1km (urban)
	15-45 km (rural)	40 km (rural)	10 km (rural)
Interference immunity	Very High	Low	Low
Proprietary or Open	Lora: proprietary;	Net: prorpietary;	open
	LoraWAN: open	Devices: open	

1 Mbps and its battery lasts from 3 to 5 years. Weightless-P covers multiple band frequencies and its battery life ranges from 3 to 8 years.

2.3 LoRa and LoRaWAN

Lora is a LPWAN modulation protocol designed for long distance communication. LoRa is the physical layer often used with the LoRaWAN MAC layer protocol. While LoRa is designed and patented by Semtech, LoRaWAN is open, non-profit and developed by the LoRa Alliance. This protocol supports bi-directional communication, mobility, localization and security required by IoT applications.

2.3.1 LoRa Modulation

LoRa modulation is based on a derivative of Chirp Spread Spetrum (CSS): a signal is spread by using wiedeband linear frequency modulated chirp pulses to encode information. It uses Frequency Shift Keying (FSK) in order to achieve lower consumption and it uses Chirp Spread Spectrum (CSS) for large area coverage. LoRa use of CSS improves resilience and robustness against interference, Doppler effect, and multipath. In CSS there are up-chrips when the frequency increases and down-chirps if the frequency decreases. These chirp signals (frequency varying sinusoidal pulses) are used as carrier signals where the message is encoded on. In addiction, the use of CSS modulation means the signals are orthogonal to each other, which allows multiple data rates simultaneously transmitting on the same channel. A representation of an up-chirp can be seen in Figure 2.1.

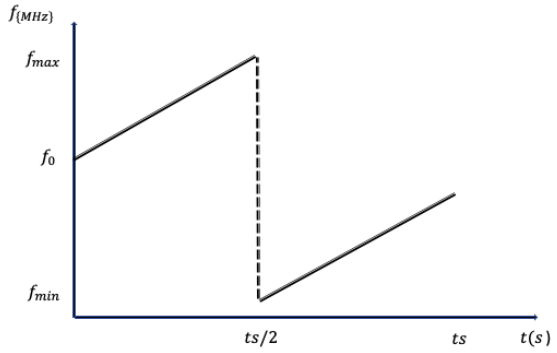

Figure 2.1: Up-chirp representation.

In LoRa, the starting frequency of a chirp, f_0, seems to be used to represent a symbol. In the case of an up-chirp, the frequency increases steadily up to f_{max}. Then it jumps back to f_{min}, growing steadily to f0 again. Afterwards, the next symbol is ready to be transmitted with a new f_0 frequency, and the process is repeated.

By examining Figure 2.1 the bandwidth, which is the number of vibrations or wave cycles per second, is given by:

$$BW = f_{max} - f_{min}, \tag{2.1}$$

Lora uses three different bandwidths:125 MHz,250 MHz,500 MHz where symbols are modulated over a chirp of a chosen bandwidth and different spreading factors are used based on data rate requirement and channel conditions. The Spreading Factor (SF) represents the number of encoded bits in a symbol and be obtained by:

$$SF = log_2(\frac{Chirprate}{Symbolrate}), \tag{2.2}$$

This also means that every symbol is encoded in 2^{SF} chirps that cover the available bandwidth. In Lora SF can assume values from 7 to 12. The symbol duartion, T_s, can therefore be expressed as:

$$T_s = \frac{2^{SF}}{BW}, \tag{2.3}$$

Considering that the symbol rate,R_s, is the inverse of T_s and that the same is related with the chip rate, R_c, by the expression:

$$R_c = R_s \times 2^{SF}, \tag{2.4}$$

Consequently. the bitrate is given by:

$$R_b = SF \times \frac{BW}{2^{SF}}, \tag{2.5}$$

It's important to highlight that by increasing the SF, the time needed for the data to be received will be longer. Therefore, the robustness of the connection will be higher but the power consumption also

increases. Another disadvantage of longer message transmission is the higher probability of collisions. This calls for a need to balance the wait time and power consumption according to the application used. The GWs have the ability of receiving data in different SFs which allows the end-nodes to choose the SF that fits better. Furthermore, the SF affects the sensitivity S of the receiver that is defined as [4]:

$$S = \text{-}174 + 10log10(BW) + NF + SNR, \tag{2.6}$$

where -174 is due to the thermal noise at the receiver in 1 Hz bandwidth, NF is the Noise Figure at the receiver (which is fixed for a hardware configuration data) and SNR is the signal to noise ratio required for the modulation.

Table 2.2 illustrates LoRa bit rates, symbol duration and sensitivity as regards to the SF.

Table 2.2: LoRa bit rates, symbol duration and sensitivity vs SF [5]

Mode	Bit rate (b/s)	Symbol duration (ms)	Sensitivity (dBm)
LoRa SF 12	293	682	-137
LoRa SF 11	537	365	-134.5
LoRa SF 10	976	204	-132
LoRa SF 9	1757	113	-129
LoRa SF 8	3125	64	-126
LoRa SF 7	5468	36	-123
LoRa SF 6	9375	21	-118

By spreading the signal in time domain it is possible to reduce the Bit Error Rate (BER) and achieve long-distance communication. LoRa can demodulate signals which are -7.5 dB to -20 dB below the noise floor.

To improve resilience against interference LoRa uses Forward Error Correction (FEC). FEC is the process where error correction bits are added to the transmitted data. The introduction of redundant data helps to restore the data when it gets corrupted. Making use of Hamming codes for FEC, LoRa offers code rates of 4/5, 4/6, 4/7, and 4/8. For example, a transmission with a coding rate of 4/5 means one bit of redundancy is added to each block of 4 bits of useful information. Code rate expression is given by:

$$CR = \frac{4}{4+n}, \tag{2.7}$$

Because of FEC coding, the number of used bits decreases, and consequently the bit rate is given by:

$$R_b = SF \times \frac{BW}{2^{SF}} \times CR, \tag{2.8}$$

2.3.2 PHY and MAC layer strucuture

At Physical layer, a LoRa frame starts with a preamble. Apart from the synchronization function, the preamble defines the packet modulation scheme, being modulated with the same SF as the rest of the packet. Typically has the duration of 12.25 T_s. There are two types of Lora packet format modes: Explicit

mode and Implicit mode. In the explicit mode after the preamble, there is an optional header. When it is present, it consists of 20 bits in total and is transmitted with a code rate of 4/8. The PHY header also contains such information as payload length, the code rate used, and whether the Payload 16-bit CRC (Cyclic Redundant check) is present in the frame. The CRC is used to detect errors in digital data. Specifically, in a LoRa network, only uplink frames contain payload CRC. In the implicit mode, the payload length, CR and CRC are fixed. The header is removed, thus reducing transmission time. The physical layer is also constituted by a payload A schematic summarizing the uplink physical frame structure can be seen in Figure 2.2.

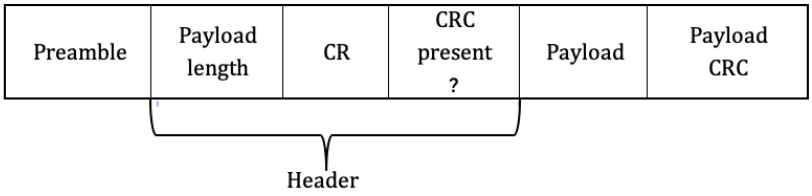

Figure 2.2: Physical layer format: Explicit mode.

The payload is sent after the header, and at the end of the frame is the optional CRC. The payload is the field that contains the actual data (51 Bytes to 222 Bytes).

The fields discussed above can also be identified looking at figure 2.3. At MAC layer frame, the packets processed consist of a MAC Header, a MAC Payload, and a Message Integrity Code (MIC). MAC header defines the protocol version and message type: whether it is a data or a management frame, whether it is transmitted in uplink or downlink, whether it shall be acknowledged. MAC Header can also notify if this is a vendor-specific message. In a join procedure for end-node activation, the MAC Payload can be replaced by join request or join accept messages. The entire MAC Header and MAC Payload portion is used to compute the MIC value with a network session key. The MIC value is used to prevent the forgery of messages and authenticate the end node.

The MAC Payload handled by the Network layer consists of a Frame Header , a Frame Port, and a Frame Payload. The Frame Port value is determined depending on the application type. The Frame Payload value is encrypted with an application session key. This encryption is based on the AES 128 algorithm.

2.3.3 Time on air

The time between a signal is sent until its reception it is called Time on air. To determine this value some formulas need to be used.

Recall the symbol duration Equation 2.3, where the bandwidth can assume the values of 125MHz,250MHz and 500 MHz and SF values from 7 to 12. Taking $n_{preamble}$ as the number of symbols in the preamble, which depends on the specifications of ISM. For Europe 863-870MHz $n_{preamble} = 8$, the $T_{preamble}$, comes as:

$$T_{preamble} = (n_{preamble} + 4.25) \times T_s, \tag{2.9}$$

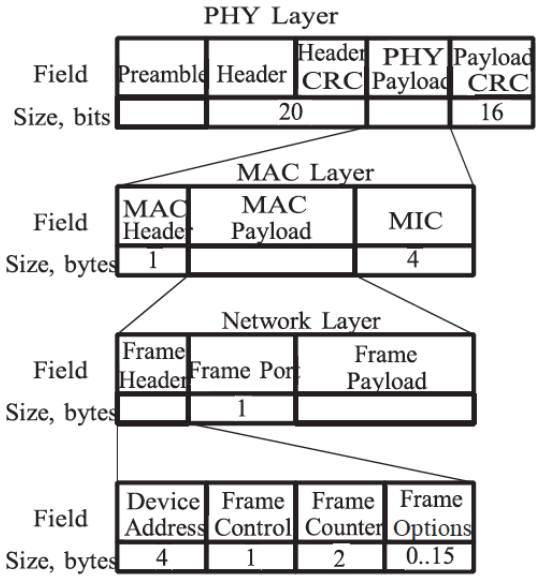

Figure 2.3: LoRaWAN frame format. [6]

Thus, to determine the duration of the payload, the following equation where $n_{payload}$ is the number of symbols in the payload, obtained by:

$$n_{payload} = 8 + max(ceil(\frac{8PL - 4SF + 28 + 16 - 20H}{4 * (SF - 2DE)})(CR + 4), 0) \tag{2.10}$$

Where PL indicates Payload size in bytes, CRC indicates the Cyclic Redundancy Check used for error detection of LoRaWAN packet. It can be either enabled (value =1) or disabled (value = 0). For LoraWAN default it is enabled. Header, H, can be implicit or explicit: H of value 0 indicates it is enabled and it is explicit mode where as H of value 1 indicates it is disabled and it is implicit mode.Low Data Rate Optimize can be enabled (Value of DE = 1) or disabled (Value of DE = 0). CR indicates Coding Rate (CR can be in the range from 1 to 4), By default it is 1

Then, the $T_{payload}$ can be obtained by:

$$T_{payload} = n_{payload} \times T_s, \tag{2.11}$$

Therefore, the equation representing Time on Air comes as:

$$TimeOnAir = T_{preamble} + T_{payload}, \tag{2.12}$$

2.3.4 Adaptive Data Rate

Recall from Section 2.3.1 that a change of the SF has implications in the data rate transmission. In order to achieve high network capacity, LoRaWAN uses the Adaptive Data Rate (ADR) mechanism developed to optimize data rates, wait time and power consumption. This mechanism consists of selecting a SF value and bandwidth for each end-node based on the collected connection metrics. This means the

SF can be changed to get better data rates for transmissions where the link is better. Furthermore, the transceivers can manage receiving different data rates in different channels.

As referred in Section 2.3.1, Lora protocol defines SFs which can take values from 7 to 12. Lowering the SF means increasing the data rate meaning lowering the Time on Air. If a node needs less Time on Air, this time can be used by other nodes to transmit. Therefore, there will be an increase on battery life preservation.

2.3.5 Specifications

Depending on the region, there are different Specifications on LoRa. The main specifications are for Europe (EU) and for the United States (US) which are listed in Table 2.3.

The minimal LoRaWAN deployment for EU in the 863-867 MHz band has 8 channels, however depending on the needs of the network this can be increased up to 16 channels.

In USA, the whole band can use 64 channels and there's a separation between uplink channels used by devices, and downlink channels used by the gateways. A subset of 8 or 16 channels can be used with a restriction on the transmission power. With more channel, a network will be able to absorb more traffic with less collisions.

Table 2.3: Europe and United States Specifications [2]

	Europe	**United States**
Frequency Rule	863-870MHz	902-928MHz
Channels	10	64+8+8
Channel BW Up	125/250kHz	125/500kHz
Channel BW Dn	125kHz	500kHz
Tx Power Up	+14dBm	+20dBm typ (+30dBm allowed)
Tx Power Dn	+14dBm	+27
SF Up	7-12	7-10
Data Rate	250bps-50kbps	980bps-21.9kpbs
Link Budget Up	155dB	154dB
Link Budget Dn	155dB	157dB

By analyzing the Table 2.3, LoRaWAN can use channels with a bandwidth of either 125 kHz, 250 kHz or 500 kHz. For these bandwidths LoRa Alliance also defines different SF and physical bit rates that can be used which are represented in Table 2.4 for the EU863-870 band:

Considering that the maximum Tx power +20 dBm can increase power consumption it's not supported by all LoRa. Instead, other values can be chosen depending on the region. Table 2.5 shows the Transmission power allowed for EU and defined by LoRaWAN. Transmission Power on a LoRaWAN device can usually be adjusted from 2 dBm to 16 dBm EIRP by step of 2 dB. A special mode called PA BOOST allows to transmit up to 20 dBm.The maximum allowed power is given by the local regulations. In Europe and most of the world, the value is 14 dBm.

Table 2.4: Bandwidths, Spreading Factor and physical rates defined by LoRaWAN for EU [5]

Data Rate	Configuration	Indicative physical bit rate (bits/s)
0	LoRa: SF12 / 125 kHz	250
1	LoRa: SF11 / 125 kHz	440
2	LoRa: SF10 / 125 kHz	980
3	LoRa: SF9 / 125 kHz	1760
4	LoRa: SF8 / 125 kHz	3125
5	LoRa: SF7 / 125 kHz	5470
6	LoRa: SF7 / 250 kHz	11000
7	FSK: 50 kbps	50000
8.. 15	RFU	440

Table 2.5: Tx powers allowed for EU [5]

Tx Power	Configuration
0	20dBm (if supported)
1	14dBm
2	11dBm
3	8dBm
4	5dBm
5	2dBm
6.15	RFU

2.3.6 Duty Cycle

Duty Cycle indicates the fraction of time a resource is busy. In Europe, duty-cycles are regulated by the ETSI standard. This standard divides 863-870 MHz band into 5 sub-bands: G, G_1, G_2,G_3 and G_4. Each sub-band has different constraints in terms of EIRP, duty cycle, and bandwidth. These limitations are defined on the Table 2.6:

Table 2.6: LoraWAN Duty Cycle regulations [7]

Name	Band [MHz]	Duty Cycle
G	863.0 – 868.0	$\geq 1\%$
G_1	868.0 – 868.6	$\geq 1\%$
G_2	868.7 – 869.2	$\geq 0.1\%$
G_3	869.4 – 869.65	$\geq 10\%$
G_4	869.7 – 870.0	$\geq 1\%$

2.3.7 LoRaWAN

LoraWAN is a Media Access layer (MAC) protocol for a high capacity star network and is implemented when the LoRa protocol is applied. As mentioned in Section 2.3.1 LoRa physical layer enables the long-range communication link. On the other hand, LoraWAN defines the system architecture and communication protocol of the network. Figure 2.4 shows LoRa distribution in the protocol layers.

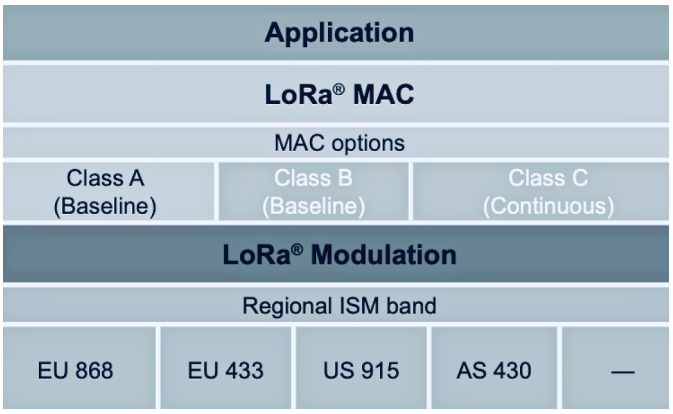

Figure 2.4: Protocol layers.[2]

2.3.8 LoRaWAN Network

LoRaWAN network architecture is usually a mesh architecture with star topology. This type of topology is the one that gives more advantages in terms of battery life of the end-nodes when long-range connectivity is achieved. Figure 2.5 shows a typical loRaWAN network composed by these type of elements:

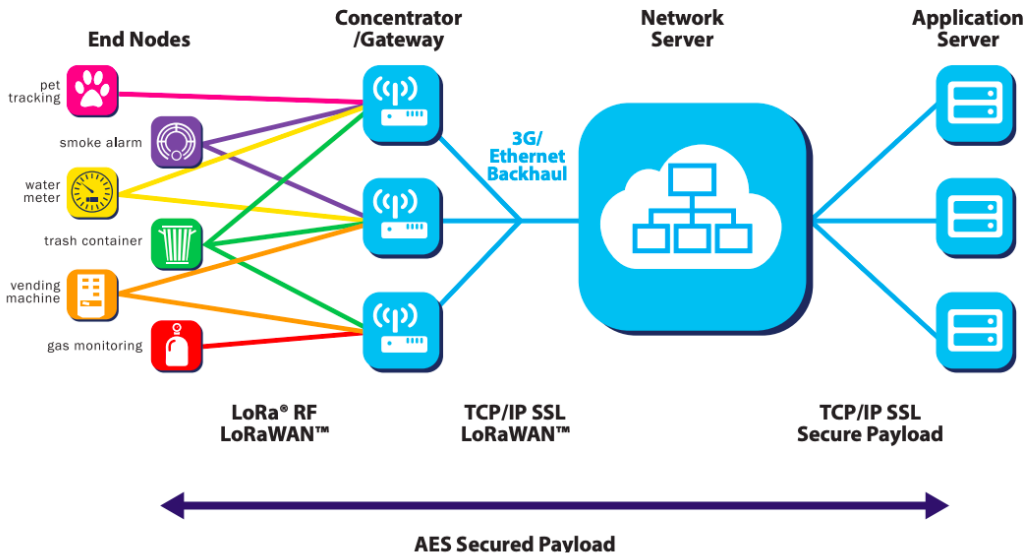

Figure 2.5: LoRaWAN Arquitecture. [2]

- **End node** - Consists of some sensor or other entity transmitting or collecting data. In the uplink scenario, the data is transmitted from the end node to the gateway. When the data is transmitted from the gateway to the end node it is called a downlink. In the LoRaWAN network, an end-node can send data to more than one gateway.
- **Gateway** - Receives the data coming from the end nodes and sends it to the network server. The connection to the server via some backhaul network(IP, Ethernet, WiFi, etc).
- **Network Server** - Collects the information from the gateway, where there is a filtering of redundancy data, the performance of security checks, and avoidance of collisions. The Network Server then forwards the information to the Application Server.
- **Join Server** - The Join Server handles the LoRaWAN join flow, including Network and Application Server authentication and session key generation.The Join Server (JS) manages the Over-the-Air (OTA) End-Device activation process. There may be several JSs connected to a NS, and a JS may connect to several NSs.
- **Aplication Server** - The final destination of the data, either in public or private clouds where the applications are running.

Looking over Figure 2.5 a particular device can be connected to more than one GW by communicating over LoRa protocol. On the other hand, the communication between a gateway and the Network Server is over TCP/IP, meaning the gateway has to be connected to the Internet in some way.

2.3.9 Device Classes

As discussed in Section 2.3 the technology support broadcast from the GWs and bidirectional communication. However, some limitations lead to the creation of different classes of endpoint devices. Depending on the use cases these are the resulted three device classes of end-devices used:

- **Class A** - Class A end devices support bidirectional communication between a device and a gateway. This Class operation is the lowest power end-device system and is the default operation mode of LoRa end devices. Figure 2.6 shows the class working mode where the end-device uplink time-slot is followed by two downlink short time-slots. The gateway can respond within the first receive slot or the second receive slot, but not both.

  Class B and C devices must likewise support class A functionality.

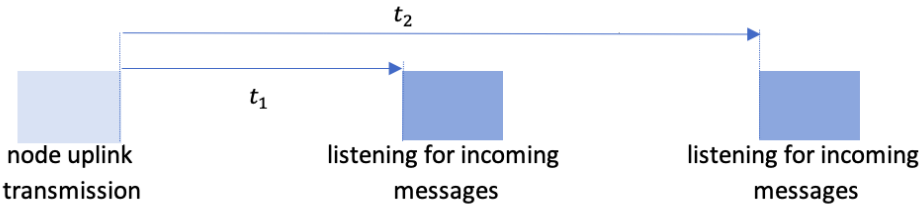

Figure 2.6: Class A working mode.

- **Class B**- In addition to random receive windows of class A, Class B devices open extra receive windows at scheduled times. This allows the gateway to knowing when the end-device is listening as represented in figure 2.8.

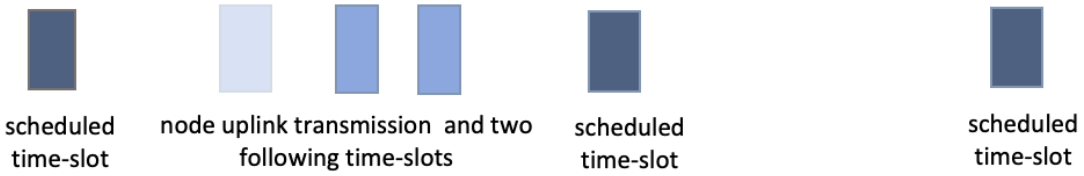

Figure 2.7: Class B working mode.

- **Class C** - In extension to Class A receive slots, Class C devices have almost-continuous open receive windows (closed when transmitting). This type of end-device use more power to operate than Class A or Class B but they offer the lowest latency for a server to end-device communication. Figure 2.8 shows class C working mode.

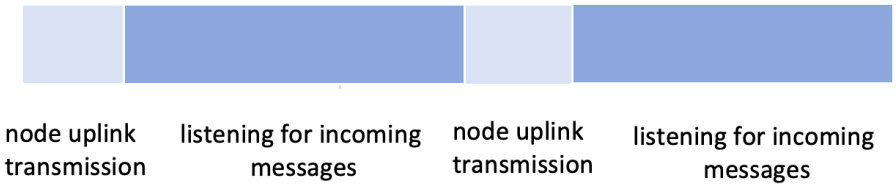

Figure 2.8: Class C working mode.

Figure 2.9 compares the main characteristics of the three class types and how they vary regarding battery lifetime and downlink latency.

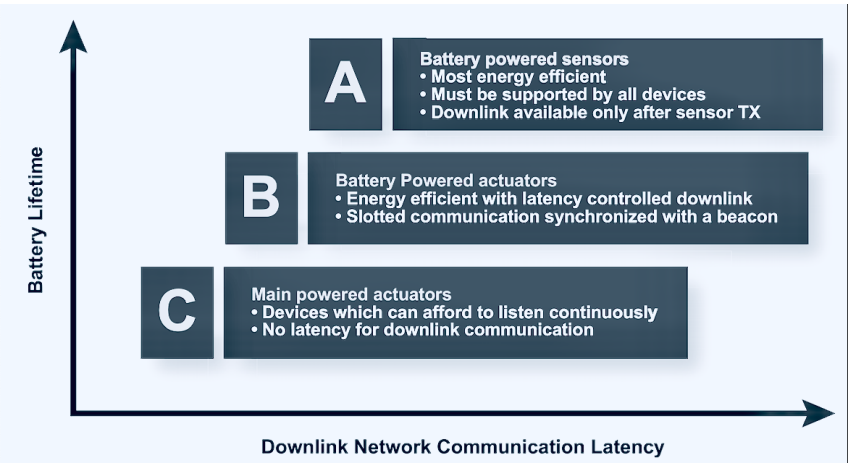

Figure 2.9: Device Classes. [2]

2.4 Multiobjective Algorithms

Most real-life science problems require a Multiobjective Optimization (MOO), which involves several conflict objectives and aims to convert all objectives into a single objective (SO) function. This conversion is usually done by aggregating all objectives in a weighted function, or transforming all but one of the objectives into constraints. This MOO has some limitations:

1) a need for *a priori* knowledge about the relative importance of the objectives, and the limits on the objectives that are converted into constraints

2) the aggregated function leads to only one solution;

3) trade-offs between objectives cannot be easily evaluated;

4) the solution may not be attainable unless the search space is convex.

The main goal of these systems is to optimize more than one objective function simultaneously and it is known as a trade-off analysis. Therefore, this MOO has many difficulties and a simple optimization process is no longer acceptable for systems with multiple conflicting objectives. In the SO optimization problem, the superiority of a solution over another solution is simply defined by analyzing their objective function values. In MO problems there is no single solution making the optimization more difficult to determine. Instead, there is a set of acceptable trade-off optimal solutions: Pareto front. The solution most desirable to the designer or decision maker (DM) is selected from the Pareto set.

Generating a Pareto set allows the DM to make an informed decision with a wide range of options since it contains the solutions that are best for all objectives. To maximize or minimize these functions a set of solutions will define the best trade off between competing objectives. MOO with M objectives can be formally described as in Equation 2.13, for a minimization problem:

$$\begin{aligned} minimize \quad & F(x) = f_1(x), f_2(x), ..., f_m(x) \\ subject \quad to \quad & g_n(x) \leq 0, n = 1, 2, ..., J, \\ & h_k(x) = 0, k = 1, 2, ...K \end{aligned} \tag{2.13}$$

2.4.1 Pareto Concepts

To compare candidate solutions to the MO problems, the concepts of Pareto dominance and Pareto optimality are commonly used.

Pareto dominance: A solution A strictly dominates solution B, when there's at least one objective in which A is better, while being no worse in all others.

Pareto optimal: A solution A is said to be Pareto optimal if and only if there does not exist another solution that dominates it. In other words, the solution cannot be improved in one of the objectives without adversely affecting at least one other objective.

Given a set of solutions, the nondominated solution set is a set of all the solutions that are not dominated by any other member of the solution set, the Pareto optimal set and the boundary defined by the set of all points mapped from the Pareto optimal set is called the Pareto optimal front. Figure 2.10 illustrates a Pareto set for a two-objective minimization problem. Potential solutions that optimize f_1 and f_2 are shown in the graph.

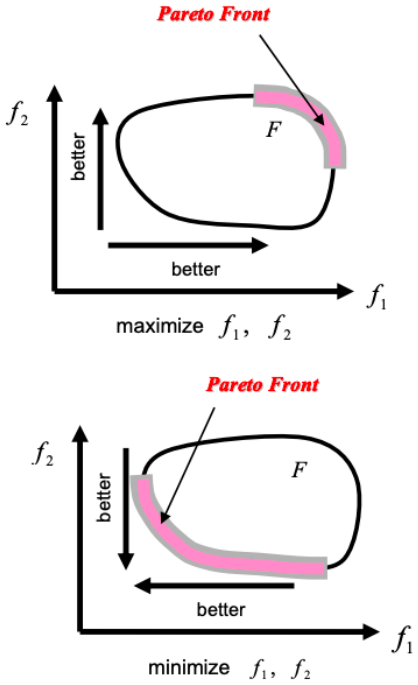

Figure 2.10: Illustration of Pareto front for a bi-objective optimization problem. [8]

In contrast to traditional mathematical programming (Weighted aggregation, Goal Programming, $E-constraint$) approaches to solve MO problems, some intelligent techniques (Evolutionary techniques)) perform direct generation of the Pareto front by simultaneously optimizing the individual objectives. In recent years, the development of computational population-based algorithms contributed to the rise of these methods.

Population-based algorithms have the advantage of evaluating multiple potential solutions in a single iteration. Also, they offer greater flexibility to decide which individuals will be part of the set of solutions, essentially in cases where no previous information is available as is the case for most real-life MO problems.

The challenge of MOO is how to guide the search towards the Pareto-optimal set, and how to maintain a diverse population to prevent premature convergence.

Evolutionary techniques that emulate the biological evolution process have been successfully applied to all sort of MOO and tend to follow the principles described above.

2.5 Multiobjective Evolutionary Algorithms

Multiobjective evolutionary algorithms (MOEAs) are widely accepted and useful for solving real-world multiobjective problems. When we have two or more conflicting objectives of a problem then we can apply MOEA. Evolutionary computing is inspired on the natural genetics and rely on bio-inspired operators such as mutation, crossover and selection where the strongest population elements are the ones that survive over the others. These methods include genetic algorithms (GA), evolutionary algorithms (EA) and evolutionary strategies (ES) which only differ in the way the fitness selection, mutation and crossover operations are performed.

Following are the steps of MOEAs:

Step1 - Initialization: initialize a random population based on the given population size.

Step2 - Fitness assignment: assign a rank to each individual of the population for generating a mating pool.

Step3 - Variation: apply variation operators (crossover, mutation) on the mating pool to generate new solutions.

Step4 - Environmental selection: select the best solutions according to the size of mating pool for next generation.

Step5 - Repeat above procedure until termination criterion is met. The following termination criteria can be used: stop after maximum number of generations, stop when algorithm succeeds in solving the problem.

MOEA generates a set of nondominated solutions at the end of run, which is called Pareto set. The Pareto front contains the set of Pareto solutions. Any MOEA aims to improve convergence of population towards true Pareto front and diversity of solutions belonging to Pareto set. The evolutionary based techniques are based on genetic algorithm.

2.5.1 Genetic Algorithm

To create a set of Pareto-optimal solutions of MOO, a first (random) set of parent solution, P_0 is created. All solutions p of that set are compared to each other and are sorted into several nondominated fronts. The first front contains all the solutions that don't dominate one another but all of them dominate the rest of solutions. Following the same logic, the solutions of the second nondominated front are dominated by the solutions of the first front, do not dominate each other, but dominate the solutions of the third front and so on. Of this first generation of solutions, only the fittest solutions are retained. The fittest solutions

are those that are closest to the Pareto front, meaning, the solutions located in the first few nondominated fronts.

These are assigned the highest rank and eliminated from further contention. The remaining individuals repeat the process until all the population is ranked and assigned a fitness value. To prevent the algorithm to converge, it is used a popular niching technique, called sharing. This technique consists of regulating the density of solutions in the hyperspace spanned by either the objective vector or the decision vector. Sharing is often used in the computation of the fitness value. Mutation and crossover operations are then performed to get the next generation of individuals (offspring). The basic flow of a GA solution is listed in Algorithm 1:

Algorithm 1: Generic GA

```
1  Start
2  Initialize population randomly (say P)
3  Define fitness function of the problem
4  Determine the fitness of the problem
5  while !Converging or Optimum not achieved do
6  |   Parent selection of the population
7  |   Crossover operation for new population generation
8  |   Perform mutation on the new population
9  |   Calculate fitness of new population
10 end
11 If optimum achieved, display the final result
12 Stop
```

There are many Genetic methods that can be used for optimization. Multi Objective Genetic Algorithm (MOGA) is a simple method where the fitness value of an individual is proportional to the number of other individuals it dominates. Sharing can be performed either in the objective space or the decision space.

Another version is the Nondominated Sorting Genetic Algorithm (NSGA), which uses a layered classification technique. All nondominated individuals are assigned the same fitness value and sharing is applied in the decision variable space. The process is repeated for the remainder of the population with a progressively lower fitness value assigned to the nondominated individuals. At their turn, these solutions are sorted into several nondominated fronts after which the process repeats itself. Because after each iteration only the best solutions of each generation are retained, the set of Evolutionary Algorithms solutions will eventually converge to the Pareto front. When after several iterations the difference between the solutions of two subsequent generations becomes negligible, it can be concluded that the Pareto front has been reached.

Figure 2.11 shows an illustration of fitness computation for NSGA in a bi-objective minimization problem. A layered classification technique is used whereby the population is incrementally sorted using Pareto dominance. Individuals in set A have the same fitness value, which is higher than the fitness of individuals in set B, which in turn are superior to individuals in set C.

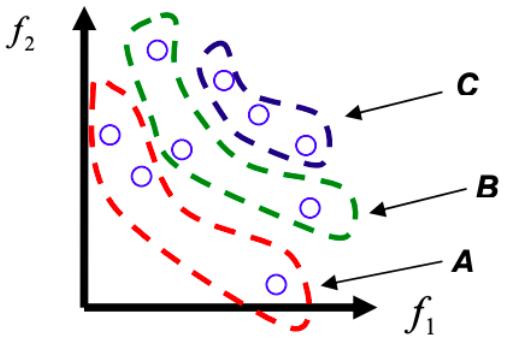

Figure 2.11: Illustration of fitness computation for NSGA. [8]

Over the years, many of these methods received criticism in their optimization approach. The lack of elitism of the algorithms described above improved promoted the development of new algorithms (SPEA, SPEA2,NSGA-II,PAES,PESA2). Since NSGA-II is the most reliable in optimizing problems with two objectives [9], a detailed description of this algorithm will be given in the next section.

2.6 NSGA-II

Multiobjective nondominated algorithms have been criticized for their computational complexity, lack of eltisim, and need for specifying the sharing parameter [10]. Nondominated Sorting Genetic Algorithm II (NSGA-II) alleviates all the difficulties mentioned above by being a fast and elitist genetic algorithm and, therefore, is the most well-known algorithm for MOO.

To entirely explain NSGA-II, some essential operations utilized throughout the optimization process need extra attention. These operations are a fast nondominated sorting approach, a crowding distance assignment, and a crowded-comparison operator. Additionally, the standard genetic algorithm operators such as binary tournament selection, simulated binary crossover and mutation are crucial for the good performance of the NSGA-II algorithm.

2.6.1 Fast nondominated sorting

Fast non-dominated sort was proposed in [10], where the time complexity is reduced compared to NSGA nondominated sorting and can be described as:

As indicated in Algorithm 2 for each solution there are two entities calculated:

1. domination count n_p: the number of solutions that dominate solution p.

2. S_p: a set of solutions that the solution p dominates.

Each solution is compared to every other solution to find out if it is dominated. In this first stage, all individuals in the first nondominated front are found and will be discounted temporarily to find the solutions in the next nondominated front. The procedure is repeated.

Analysing the sorting equations, in the first nondominated front, all solutions are initialized with an

empty domination count. Now, for each solution p with n_p=0, we visit each member (q) of its set S_p and reduce its domination count by one. While doing so, if for any member the domination count becomes zero, we put it in a separate list Q. These members belong to the second nondominated front. Following that, the above procedure is continued with each member of Q and the third front is identified. This process continues until all fronts are identified.

Algorithm 2: Fast nondominated sorting (P)

```
for each p ∈ P
    S_p = ∅
    n_p = 0
    for each q ∈ P
        if (p ≺ q) then                          ▷ If p dominates q
         S_p = S_p ∪ q;                          ▷ Add q to the set of solutions dominated by p
        else if (q ≺ p) then
         n_p = n_p + 1                           ▷ Increment the domination counter of p
    if n_p = 0 then                              ▷ p belongs to the first front
        p_rank=1
        F_1= F_1 ∪ p
i=1                                              ▷ Initialize the front counter
while F_i ≠ ∅
    Q = ∅                                        ▷ Used to store the members of the next front
    for each p ∈ F_i
        for each q ∈ S_p
         n_q = n_q - 1
         if n_q = 0 then                         ▷ q belongs to the next front
          q_rank =i+1
          Q = Q ∪ q
    i = i + 1
    F_i = Q
```

2.6.2 Crowding distance

In addition to the nondominated sorting, which arranges the population according to fitness, crowding distance assignment is performed in order to determine the diversity among the different solutions in the population. This means that crowding distance is a parameter calculated for each individual used to measure how close an individual is to its neighbors.

In GAs, it is desirable to preserve a spread of solutions within the search space. In terms of diversity preservation, NSGA-II also claims to be significantly improved compared to NSGA, which depended on the sharing parameter requiring user input. Thus, causing the necessity of a comprehensive comparison among the solutions in the population, resulting in a quite high computational complexity. The improved NSGA-II avoids these challenges by introducing the crowded-comparison approach, not requiring any user input while reducing computational complexity. Moreover, the crowding distance, $i_{distance}$, is computed within each nondominated front in the population. This is done by sorting the solutions within each front according to each objective function value in ascending order of magnitude. Next, for each objective function, boundary solutions, the smallest and largest function value are assigned an infinite distance value, $i_{distance} = \infty$. All intermediate solutions are assigned a distance value for each objective function, equal to the normalized corresponding objective function values of two adjacent solutions. Summing up,

the crowding distance is calculated individually for each objective function. Finally, the overall crowding distance is calculated as the sum of the individual distances corresponding to each objective.

Figure 2.12 illustrates the crowding distance of the *i*th in its front (marked with solid circles) is the average side length of the cuboid (shown with a dashed box). Note that points marked in filled circles are solutions of the same nondomination front. Although Figure 2.12 calculates the crowding distance for two objectives, the procedure is applicable for more than two as well.

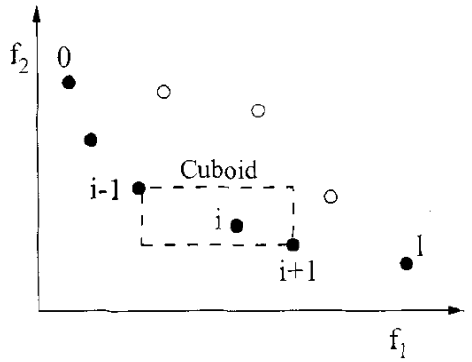

Figure 2.12: Crowding distance calculation. [10]

Algorithm 3 outlines the crowding-distance computation procedure of all solutions in an nondominated set .

Algorithm 3: Crowding distance assignment

1 $\mathcal{J}$ = $|\mathcal{I}|$ ▷ number of solutions in $\mathcal{I}$

2 for each i, set $\mathcal{I}[i]_{distance}$=0 ▷ Initialize distance

3 for each objective m

4 $\mathcal{I}$ = sort ($\mathcal{I}$, m) ▷ sort using each objective value

5 $\mathcal{I}[1]_{distance} = \mathcal{I}[\mathcal{J}]_{distance} = \infty$ ▷ So that boundary points are always selected

6 for i = 2 to ($\mathcal{J}$ - 1) ▷ for all other points

7 $\mathcal{I}[i]_{distance} = \mathcal{I}[i]_{distance} + (\mathcal{I}[i+1].m - \mathcal{I}[i-1].m) / (f_m^{max} - f_m^{min})$

In this procedure, *I* refers to the *m*th objective function value of the *i*th individual in the set *I* and the parameters f_m^{max} and f_m^{min} are the maximum and minimum values of the *m*th objective funtion.

After all population members in the set *I* are assigned a distance metric, we can compare two solutions for their extent of proximity with other solutions. A solution with a smaller value of this distance measure is, in some sense, more crowded by other solutions. This is exactly what we compare in the proposed crowded-comparison operator, described below.

2.6.3 Crowding comparison operator

After performing the nondominated sorting and the crowding distance calculation, the crowded comparison operator can be defined. The crowded comparison operator ($\prec_n$) is used for the selection once the individuals are sorted based on nondomination and with crowding distance assigned. Therefore, assuming

every individual i in the population has two attributes:

1. nondomination rank (i_{rank});
2. crowding distance ($i_{distance}$) ;

   We now define a partial order $\prec_n$ as

   $i \prec_n$ if ($i_{rank} < j_{rank}$) or (i_{rank} = j_{rank}) and ($i_{rank} > j_{rank}$)

The crowded-comparison operator compares two solutions for their extent of proximity to other solutions. It also takes rank into account, as lower (better) ranks are preferable. If two solutions have the same rank, the solution located in a less crowded region, that is, the solution with the higher crowding distance is preferred.

2.6.4 Binary tournament selection

In general, tournament selection consists of choosing a number t of individuals at random from the population and copying the best individuals from the group of t individuals into the intermediate population. t is known as the tournament size, and such tournaments are often held between two individuals. Tournament selection with t = 2 is called binary tournament selection. As briefly mentioned, the remaining slots of the next parent population correspond to solutions selected by binary tournament selection based on the crowded comparison operator, forming P_{t+1} of size N. Thus, two solutions from the front that cannot be entirely resided in P_{t+1} are contending against each other, and the solution with the largest crowding distance is transmitted into P_{t+1}.

2.6.5 Main loop

As described in Section 2.5 based on the problem range a random parent population P_0 is created. Once the population is initialized, the population is sorted based on the nondomination into each front. The first front contains the elements which are completely nondominated in the current population and the second front the elements which are dominated by the set of individuals in the first front only and the front goes so on. Individuals in each front are assigned a fitness (or rank) value based on the front in each they belong to. Individuals in first front are given a fitness value of 1 (best level) and individuals in second are assigned fitness value as 2 (next-best level) and so on.

In addition to fitness value, crowding distance is calculated for each individual measuring how close an individual is to its neighbors. Large average crowding distance will result in better diversity in the population.

At first, the usual binary tournament selection, recombination, and mutation operators are used to create a offspring population Q_0 of size N. After the initial generation the process is different since it introduces elitism by comparing the current population with the previously found best nondominated solutions.

Algorithm 4: make new population (P_{t+1})

1 R_t=$P_t \cup Q_t$ ▷ combine parent and offspring population
2 $\mathcal{F}$ = fast non dominated sort (R_t) ▷ $\mathcal{F}$ = ($\mathcal{F}_1$, $\mathcal{F}_2$,...), all nondominated fronts of R_t
3 P_{t+1} = $\emptyset$ and i = 1
4 until | P_{t+1} | + | $\mathcal{F}_i$ | $\leq N$ ▷ until the parent population is filled
5 crowding distance assignment ($\mathcal{F}_i$) ▷ calculate crowding distance in $\mathcal{F}_i$
6 P_{t+1} = $P_{t+1} \cup \mathcal{F}_i$ ▷ include ith nondominated front in the parent pop
7 i = i + 1 ▷ check the next front for inclusion
8 Sort ($\mathcal{F}_i$, $\prec_n$) ▷ sort in descending order using $\prec_n$
9 P_{t+1} = $P_{t+1} \cup \mathcal{F}_i$[1: ($N$ - | P_{t+1} |)] ▷ choose the first (N - | P_{t+1} |)elements of $\mathcal{F}_i$
10 Q_{t+1} = make new pop (P_{t+1}) ▷ use selection, crossover and mutation to create a new population
11 t = t + 1 ▷ increment the generation counter

The proposed algorithm that describes next generation procedure is shown in Algorithm 4. Also, by analysing Figure 2.13 a combined population R_t=$P_t \cup Q_t$is formed. The R_t population, of size 2N is sorted according to nondomination with elitism ensured as it contains all individuals of P_t and Q_t. The solutions that belong in front F_1 are the best ones in the combined population. If the size of F_1 is smaller than N we chose all the elements of this set for the new population P_{t+1}.

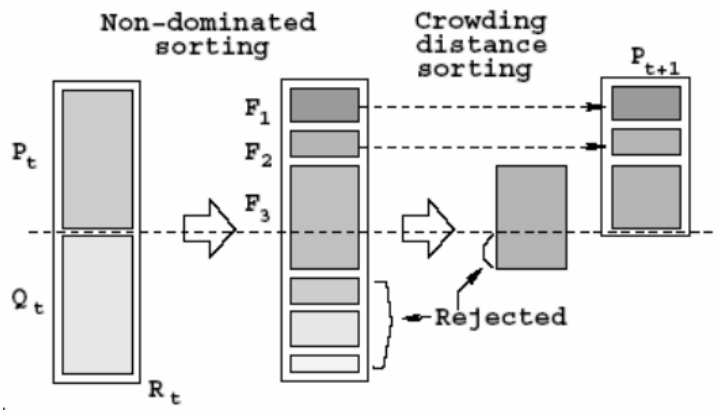

Figure 2.13: NSGA-II procedure.[10]

The remaining elements will be chosen, from the next nondominated fronts in order of their ranking. Members from front F_2 will chosen before members from front F_3 ans so on. This procedure will continue until no more sets can be accomodated. To choose exactly N population members, we sort the solutions of the last front using the crowded-comparison operator ($\prec_n$) in descending order and choose the best solutions needed to fill all population slots. The new generation P_{t+1} is now ready for selection, mutation, crossover to create a new population Q_{t+1}. It is important to note that we use a binary tournament selection operator but the selection criterion is now based on the crowded-comparison operator ($\prec_n$).

As referred previously, the individuals are selected by using a binary tournament selection with crowed-comparison-operator. We prefer the solution with the lower (better) rank. Otherwise, if both solutions belong to the same front, than we prefer the solution that is located in a lesser crowded region.

Since this operator requires both the rank and crowded distance of each solution in the population, we calculate these quantities while forming the population P_{t+1}, as shown in Algorithm 4.

These are the three main innovations for the NSGA-II algorithm: a fast nondominated sorting procedure that ensures elitism, a fast crowded distance estimation procedure, and a simple crowded comparison operator that guarantees diversity preservation and estimation.

2.7 Related work on Smart Metering Network Optimization

As the emerging networking technology for IoT, LoRaWAN has gained a significant amount of focus from researchers around the world. In this section, we briefly review some of the existing studies about LoRaWAN performance.

A study in [1] investigates a LoRa wireless network deployment for electricity metering, where this technology was combined with an event-based metering strategy. The study proposed a stochastic geometry model including a density of external interferers and a random SF allocation. The results showed that the outage probability is affected by the interference and the smart meter - gateway distance. Also, the event-based strategy usually exceeds the time-based in terms of reconstruction error. It is worth to highlight that, although the results are based on realistic numbers and actual electricity demand data, they are used here to test a concept that must be further analyzed and optimized. Even with the particularities of each specific application, in general, LoRa combined with an event-based sampling strategy leads to a fairly good quality signal reconstruction. Additionally, it provides a scalable solution for massive machine-type communications and IoT deployments needed in the future smart cities.

Another study in [11] investigated the employment of wireless technologies for SG application. The research showed that from low installation costs to an easy implementation of the communication network there are numerous advantages in integrating this model solution. Although LoraWAN doesn't have a part in the study, wireless technologies are the primary candidates for the success of a SG communication network. However, the study results prove that a combination of mixed and wired technologies may introduce latencies and future works must plan improvement of the ICT model.

The work in [12] studied the performance of a LoRa-based IoT network in a typical urban scenario. To simulate a whole LoRa network, a system level simulator in ns-3 was implemented, where the tests estimated throughput, packet error probability, and GW coverage. Having a realistic urban propagation scenario, with streets and buildings in account, the results presented demonstrate that a LoRaWAN network provides a higher throughput than a typical ALOHA-based scheme, thanks to the new access scheme it employs (partial orthogonality between its SFs). Additionally, simulation results show that a LoRa network can scale well, mainly because an increase in the number of GWs improves the coverage and reliability of the uplink as well. The simulation of the network resulted in achieving packet success rates above 95%.

In conclusion, this study aims to optimize the GWs positions to provide a high-quality throughput between devices. Since the LoraWAN network provides good quality signal this study will be focused on it's deployment optimization.

Chapter 3

LoRaWAN Performance Evaluation Tools

This chapter presents the theoretical LoRa model that was implemented in Matlab. All the propagation models, packet error models, parameters choices and how fading and shadowing were estimated are explained.

3.1 LoRaWAN Analytical Model

The LoRaWAN model developed in this study is based on the INESC-ID model developed in the WimeCom project [13]. This model allows the computation of the Signal-to-Interference-plus-Noise-Ratio (SINR) and Packet Loss Ratio (PLR) for each device in a LoRaWAN network of Class A devices that may involve several gateways and support more than one frequency band. In the following sections, a detailed explanation of the propagation model and packet error model is provided.

Large Scale and Small Scale Fading

Before explaining in detail the analytical model used in this thesis, a taxonomy of fading effects must be presented.

A transmitted signal undergoes changes while traveling through the propagation path to the receiver. The effect of these changes is commonly called fading. In free-space, a signal follows one path and arrives at the receiver with an attenuation that is proportional to the square of the distance. This is not the case for a signal that encounters obstacles in the propagation path. Instead, the signal is reflected, diffracted, and scattered from objects that are present in the path. Each path can be subject to different amounts of attenuation, delay, and fading type. At the receiver, the signals can add constructively or destructively, depending on phase relationships, causing random and rapid fluctuations in the received amplitude when the receiver or the transmitter is moving. Due to the Doppler effect, this situation also causes the signal to be spread in the frequency domain. However, Doppler effect will not be considered

in this study.

The fading phenomena can be classified into two main groups known as large scale fading and small scale fading. The large scale fading is used to describe the signal level at the receiver after traveling over a large area (hundreds of wavelengths). Large-scale fading is the result of signal attenuation due to signal propagation over large distances and the blocking effects of large objects in the propagation path.One effect studied in this master thesis, Path Loss, loss due to distance, occurs when part of the reflected signal is lost. This channel effect corresponds to large-scale fading.Shadowing is also considered large-scale fading. Log normal shadowing is the result of the signal being blocked by large objects in the propagation path. These are typically distant objects in the environment such as mountains, hills, or large buildings. The statistical model used to describe shadowing is the log-normal distribution of the mean signal power. A detailed explanation of shadowing effect in Section 3.2.2.

Small scale fading is used to describe the signal level at the receiver after encountering obstacles near the receiver (several wavelengths to fractions of wavelengths). Two common small-scale fading models are Rayleigh and Rician. This study will only consider Rayleigh fading and a detailed explanation of this effect will be given in Section 3.2.3. A representation of fading classification is illustrated in Figure 3.1.

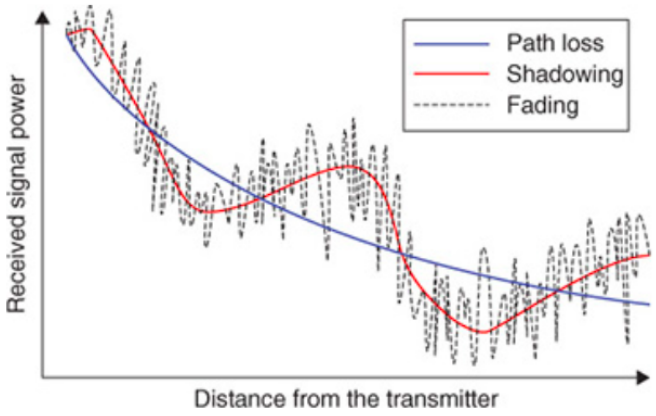

Figure 3.1: Representation of the large-scale (distance-dependent path loss and shadowing) and small-scale (fading) propagation effects. [14]

3.1.1 Signal reception model and selection of spreading factors

This thesis assumes a log-distance path loss model, in which the received power P_r is given by the following expression:

$$P_{r[dBm]} = P_{t[dBm]} - PL_0 - 10.a.log_{10}\frac{d}{d_0} + 20.log_{10}(\alpha) + X(\sigma) \tag{3.1}$$

where P_t is the transmit power, PL_0 is the path loss at reference distance d_0, a is the path loss exponent, d is the distance between the device and the gateway, α represents the Rayleigh fading, is a random variable with exponential distribution and $E(\alpha^2) = 1$, and $X(\sigma^2)$ is a Gaussian random variable,

modeled as log normal, with zero mean and variance parameter σ^2.

In the first part of this study, in order to simplify the model, the terms related with fading and shadowing were not included, so that P_r [dBm] becomes deterministic.

Furthermore the effects of shadowing and fading will be included and an explanation of it's calculation for the propagation gain will be given in Section 3.2. Therefore, to calculate log-distance path loss we only consider the elements of the following equations:

$$P_{r[dBm]} = P_{t[dBm]} - PL_0 - 10.a.log_{10}\frac{d}{d_0} \tag{3.2}$$

The value of PL_0 in Equation 3.2 used to be based on a free space calculation or experimental measurements performed at the distance of reference, $d0$. Considering project WiMeCOM [13] empirical parameters, the value used in this study is 8.1dB. In this model the receiver sensitivity is taken into account when choosing the SF, it being considered that the device will employ the lowest SF possible:

$$SF_i = \min_g(j|P_{r^i g} \geq RS_j), \tag{3.3}$$

where SF_i is the SF chosen by device i, Pr_i^g is the received power from device i at gateway g, and RS_j is the receiver sensitivity associated with spreading factor j. In this study, the allocation of SF depends on the distance to the GWs and the propagation model that is used.

Pathloss exponent

The following Table 3.1 contains the values for the path loss exponents in different environments. In this master thesis the LoRaWAN model is analysed in a simulating shadowed urban cellular radio environment.

Table 3.1: Path loss exponent [15]

Environment	Path loss exponent
Free Space	2
Urban area cellular radio	2.7 to 3.5
Shadowed urban cellular radio	3 to 5 dB
In building line of sight	1.6 to 1.8
Obstructed in buildngs	4 to 6
Obstructed in facotries	2 to 3

3.1.2 Packet error model taking into account a single gateway

The packet loss model for the case of a single gateway was modeled in two ways. The first approach calculates the distribution of the total interfering power as the convolution between the probability distribution functions of the possible interfering devices. Then, it calculates the Signal-to-Interference-Ratio (SIR) distribution. Due to the computational complexity of this approach, another model was

developed, which computes the packet loss probability based on the collision probability and average SIR during collision. Both models make the following assumptions:

1. The packet error rate depends only on the SIR, being independent of the specific fields of the packet that are affected by interference.

2. Interference occurs only between transmissions using the same channel and SF. Different SFs are orthogonal.

3. All the packets have the same duration T_{tx}.

3.1.3 Packet error model based on a collision model

Sub-band occupancy and delay model

A LoRaWAN device may choose among different available sub-bands. Spectrum utilization regulations impose duty cycles that limit the load imposed by a device on each sub-band. Also, different sub-bands may have a different number of channels. If one assumes that a device chooses the transmission channel according to a uniform distribution over all the available channels just before transmission, utilization of the sub-bands will be asymmetric. These characteristics are taken into account in the work of René Søresen et al [16]. The model assumes a Poisson process of packet generation. According to this model, the total transmission latency is given by:

$$T_{total} = T_{tx} + T_{w'} \tag{3.4}$$

where T_{tx} is the time-on-air of the packet and T_w is the waiting time due to duty-cycling. T_tx can be calculated according to the LoRaWAN specification, based on the payload length, SF, channel bandwidth, code rate and protocol overhead. Since different sub-bands may have different regulatory duty-cycles, an asymmetric M/D/c queuing model is considered, with c denoting the number of available sub-bands, which in practice is approximated by a jockeying M/M/c queue. An empirical assumption is made that the waiting line of the M/M/c queue is approximately twice that of an M/D/c queue. Knowing the packet rate λ produced by a device, T_w can thus be calculated based on Little's Law:

$$T_w = \frac{p_{busy,all}}{(\sum_{i=1}^{c} \mu_i - \lambda).2'} \tag{3.5}$$

where $p_{busy,all}$ is the Erlang-C probability that all sub-bands are busy and $_i$ is the service rate of sub-band i. The service ratio of a sub-band i, r_i is given by the following expression:

$$p_i = \frac{\mu_1}{\lambda}.(1 - p_{i,idle}) \tag{3.6}$$

The jockeying M/M/c queue is used to calculate $p_{busy,all}$ and $p_{i,idle}$.

Collision model

In order to determine the total traffic load and collision probability, the sub-band occupancy model [16] is used. Based on this model, for each sub-band s and SF j in a gateway, the total traffic load is calculated as follows:

$$L(s,j) = \frac{\lambda.p_s.T_{txj}.N.p_{SF_{s,j}}}{n_s} \tag{3.7}$$

where p_s is the service ratios of the sub-bands, T_{tx} is the time-on-air of the packet, p_{SF} is the percentage of devices N using spreading factor j in sub-band s and n_s is the number of channels in sub-band s.

Based on a simple ALOHA model, the probability of collision can be calculated as:

$$p_{col,s,j} = 1 - e^{-2L(s,j)} \tag{3.8}$$

The model defined in [16] assumes that a packet is lost every time there is a collision. However, this doesn't take into account capture effects, with the possibility of successful packet reception in case the received powers of the colliding packets being too different. This would result in a SIR that is high enough for one of the packets to be received. As such, an extension of the collision model was developed, which takes SIR into account. Regarding manageability, the model assumes that the probability of collision between more than two transmissions is not significant compared to the probability of collision between two transmissions. Hence, only collisions between two transmissions are considered.

The average SIR resulting from a collision is calculated based on the average interference power during transmission of the reference packet represented in Figure 3.2.

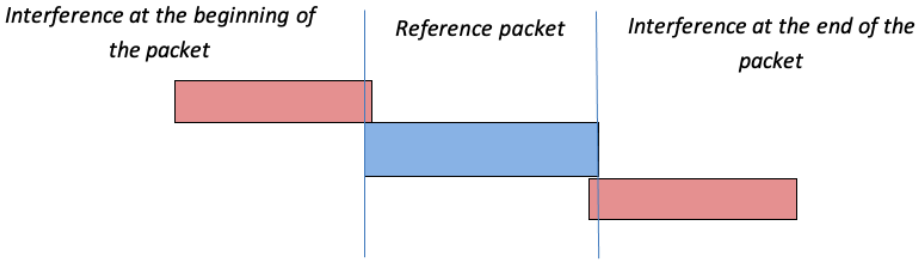

Figure 3.2: Overlapping between two packets during a collision.

Since, according to the ALOHA model, the starting times of interfering packets are uniformly random within the vulnerable period of $2.T_{tx}$, it is considered that the average interfering power is one half of the instantaneous power received from the interfering node:

$$SIR_{i,s} = \frac{P_{r_i}}{\frac{\sum_{l=1}^{N} 1_{l \neq i \wedge SF(l)=SF(i)^{(l,i)}.\frac{P_{rl}}{2}}}{\sum_{l=1}^{N} 1_{l \neq i \wedge SF(l)=SF(i)^{(l,i)}}}}, \tag{3.9}$$

Where $SIR_{(i,s)}$ is the average SIR of the reception of a packet from device i in sub-band s and $1_{l \neq i \Lambda SF(l)=SF(i)}$ is an indicator function to limit the interfering nodes to those who employ the same SF. Again, it is considered that the packet is lost when $SIR_{(i,s)} <$ 6 dB.

The average PER of packets transmitted from node i to a gateway g is then estimated as follows:

$$P_{e\,g}^{i} = \frac{\sum_{s=1}^{N_s} \sum_{i=1}^{N} 1_{<6dB}(SIR_{i,s}).p_s}{N.S} \tag{3.10}$$

3.1.4 Packet loss model with multiple gateways

When there are multiple gateways within range of a device, the packet loss probability tends to lower, since it is enough that at least one gateway receives the packet in order for the transmission to be successful. The Packet Loss Ratio (PLR) is thus the probability that all gateways have received the packet with errors. If it is assumed that the PERs of different gateways are independent (best case), PLR of device i is calculated as follows:

$$PLR_i^{min} = \prod_{g=1}^{N_G} P_{e\,g'}^{i} \tag{3.11}$$

where N_G is the number of gateways (it should be noted that for gateways out-of-range from the device, $P_e^{i_g} = 1$) . However, the PERs of different gateways are not independent, since some interfering device that causes a collision in one gateway may also interfere at the same time with the reception of the same packet in other gateways. Consequently, at the other extreme, the PLR estimate corresponds to the minimum PER of all the gateways:

$$PLR_i^{max} = \min_{g} P_e^{i'_g} \tag{3.12}$$

3.2 Fading and Shadowing model

The propagation model described in Section 3.1 predicts the received power as a deterministic function of distance, where the communication range is represented as an ideal cycle.

Experimental results have shown that many well-designed protocols will fail simply because of fading and shadowing experienced in a realistic wireless environment. This section aims to explain how this thesis adopts a typical LoRaWAN operating scenario where the transmissions of LoRa Class A devices are affected by path-loss, shadowing and fading. With the purpose of evaluating LoRa's performance in large and small scale fading environments, we consider both Rayleigh fading and Lognormal shadowing.

3.2.1 Fading

Fading is caused by movement of transmitter, receiver or other object in the environment. A Rayleigh distribution is normally used to describe the statistical time-correlation nature of the received signal envelope, or the envelope of an individual multipath component. When there is a dominant stationary (non-fading) signal component present, such as line-of-sight (LOS) propagation path, the small scale fading envelop distribution is Ricean [17]. In this study, only Small scale fading following Rayleigh distribution will be considered for the simulation results, considering that you rarely have a dominant LOS ray in a typical LoRaWAN network.

Fading channel can be characterized by a random variable α that describes random nature of envelope fading. Since the performance of wireless communication systems is mainly function of signal to noise ratio, the fading level has to be described in power. Hence, Rayleigh amplitude fading channels can be described as exponential fading distribution in power domain.

The amplitude of a signal subject to fading is assumed to be distributed according to a Rayleigh distribution. Therefore, the power of the fading effect distributed according to an Exponential distribution. The shorthand $X \sim \text{exponential}(\alpha)$ is used to indicate that the random variable X has the exponential distribution with positive scale parameter α. The exponential distribution can be parameterized by its *mean* α with the probability density function

$$f(x) = \frac{1}{\alpha} e^{-x/\alpha} \qquad x > 0,$$

for $\alpha > 0$. An exponential random variable X can also be parameterized by its *rate* λ via the probability density function

$$f(x) = \lambda e^{-\lambda x} \qquad x > 0,$$

for $\lambda > 0$.

Regarding this thesis research the distribution of power in the receiver is an exponential distribution. This means, because of fading effect the power at the receiver due to path loss, will lead to the instantaneous power at the receiver having the probability distribution explained above.

Therefore, this propagation model can be represented by Equation 3.13.

$$P_{r[dBm]} = P_{t[dBm]} - PL_0 - 10.a.log_{10}\frac{d}{d_0} + 20.log_{10}(\alpha) \tag{3.13}$$

Where α, Rayleigh fading, is a random variable with exponential distribution and E(α^2)=1

3.2.2 Shadowing

Additionally to the fading effect, the log-distance path loss propagation model doesn't consider the fact that the surrounding environmental clutter may be vastly different at two different locations having the same T-R separation. This leads to measured signals which are vastly different than the average value predicted by Equation 3.2 in log-distance path loss model. Measurements have shown that at any value of d , the path loss $PL(d)$ at a particular location is random and log-normally distributed about the mean distance-dependent value. This is given by Equation 3.14.

$$P_{r[dBm]} = P_{t[dBm]} - PL_0 - 10.a.log_{10}\frac{d}{d_0} + X(\sigma) \tag{3.14}$$

The log-normal distribution describes the random shadowing effects which occur over a large number of measurement locations which have the same T-R separation, but have different levels of clutter on the propagation path.

This phenomenon is referred to as log-normal shadowing. Simply put, log-normal shadowing implies that measured signal levels at a specific T-R separation have a Gaussian (normal) distribution about the distance-dependent mean of Equation 3.14 in Log-distance Path Loss model, where the measured signal levels have values in dB units.

The standard deviation of the Gaussian distribution that describes the shadowing also has units in dB. Thus, the random effects of shadowing are accounted for using the Gaussian distribution which lends itself readily to evaluation.

In this model, the values of n, and σ are based on empirical results.

3.2.3 Fading and shadowing model validation

For the implementation of fading and shadowing effects some validations were made in Matlab to ensure the models of propagation were giving the expected results.

Fading

As explained in previous sections the fading effect follows an exponential distribution with a detailed description in Section 3.2.1. When Lora's theoretical parameters were used to generate this distribution, the following results were obtained. First, the random samples of power received signals with fading are represented in Figure 3.3.

Additionally, a histogram represented in Figure 3.4, guarantees these samples follow an exponential distribution. This ensures that our fading propagation model will correctly provide different instances of signal propagation.

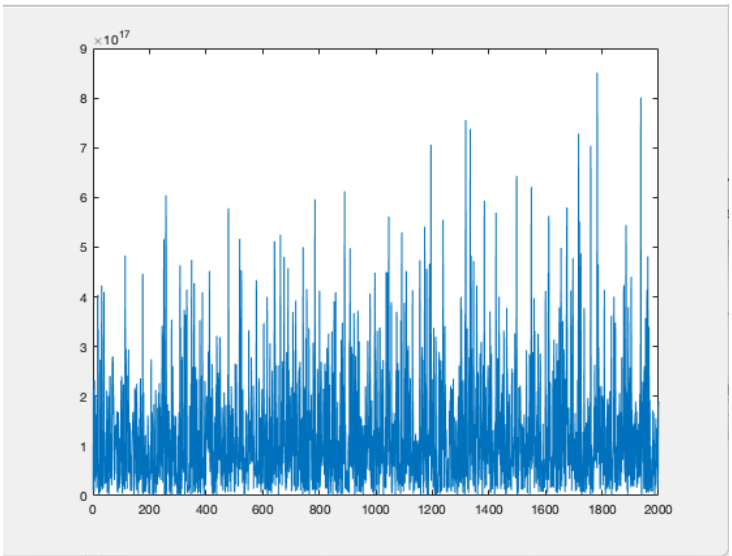

Figure 3.3: Exponential Random Samples.

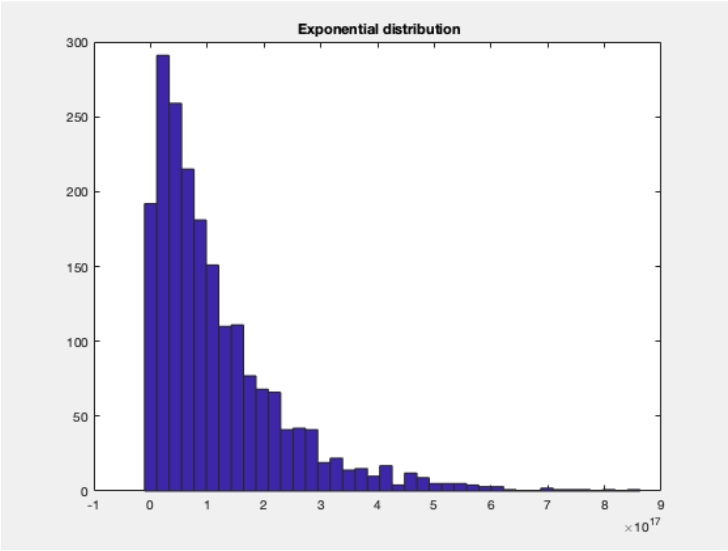

Figure 3.4: Histogram of the received power probability distribution for the Rayleigh fading channel.

Shadowing

The validation of the propagation model in the previous section was also performed for the shadowing propagation model. First, we generated random samples following log-normal shadowing, as represented in Figure 3.5. Then, using Matlab histogram function, the samples led to a normal distribution. This result, guarantees that the instances of signals generated with shadowing propagation model will be correct. Figure 3.6 and Figure 3.7 illustrate the normal distribution of the samples with different parameter values.

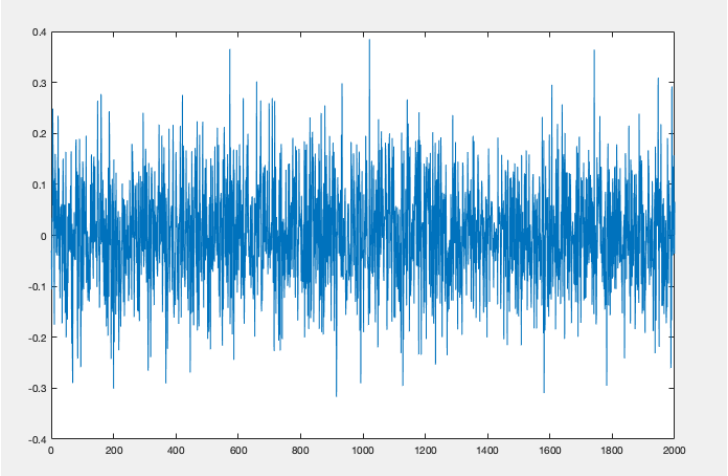

Figure 3.5: Samples of random numbers generated from normal distribution.

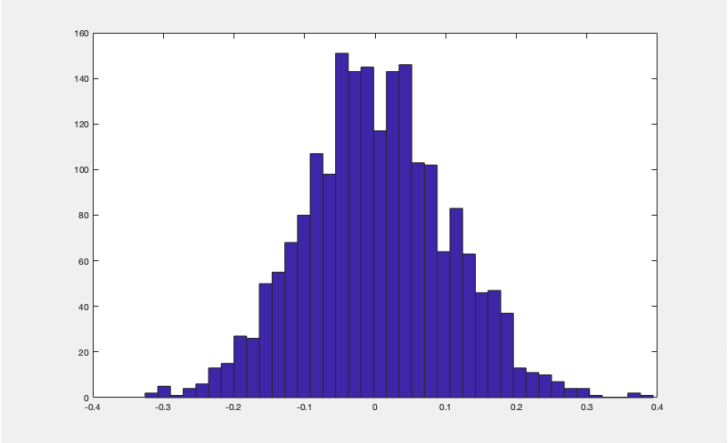

Figure 3.6: Log-normal distribution $\sigma = 0.1$.

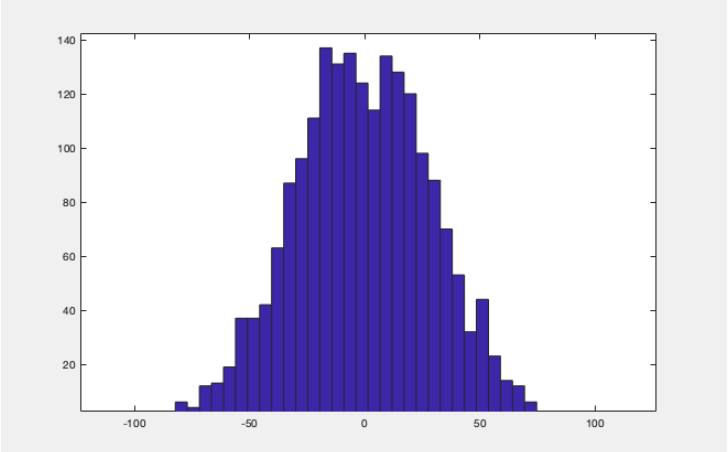

Figure 3.7: Log-normal distribution $\sigma = 30$.

Chapter 4

LoRaWAN Gateway Placement Optimization for Smart Metering Infrastructures

The objective of this thesis is to optimize the deployment of a SM network using a LoRaWAN solution. It is assumed that the locations of SM devices is an input to the problem. The objective is then to find the best trade-offs between the cost of the investment on network infrastructure and the quality of the connectivity. For this accomplishment, NSGA-II algorithm explained in Section 2.6 was developed in Matlab also based on the model developed in the WimeCom project [13]. A detailed explanation of the model complementing the operations on the same section will be given.

4.1 Objective Functions

As already stated, the developed algorithm seeks to find the best trade-offs between the minimum cost for investment on the infrastructure and the quality of connectivity.

Analytically, this tasks aim for a balance between the number of GWs and number of loss packets. For this effect, the OFs should be the following:

OF_1: $\min Gw$

OF_2: $\min avg\ p_{loss}$

where G is the number of GWs and p_{loss} the average of the number of loss packets. The number of lost packets can be calculated based on the computation of the collision probability for ALOHA systems.

Since the OFs are defined, the NSGA-II algorithm can be executed. To understand the complete process of NSGA-II, some detail about the algorithm's operations will be given in the next sections.

4.1.1 Initialization and Stopping Criteria

NSGA-II starts by generating an initial population set according to the propagation model that is used. In fading or shadowing model the population is initialized assuming an average of 5 channel instances of the received power. With Log distance model the initial population stars without this channel instances calculation.

The first population is used to generate offspring chromossomes using the geneting operations explained in Section 4.1.3 and Section 4.1.4. These chromossomes are merged and sorted in order to select the non-dominated solution to be used in the next generation.

The outputs of the algorithm are monitored and analysed every 10 iterations. The algorithm stops if there isn't a change in the population of the candidate solution. This means that if the Pareto optimal Curve contains the same solution for 10 consecutive iterations it's assumed that the algorithm has converged, and therefore, the simulation is finished.

4.1.2 Individual Chromosome

An individual encodes a candidate solution to the problem and it corresponds to an instance of a structure called chromosome. Each gene of the chromosome encodes an independent variable. The chromosome defined for this problem is depicted in Figure 4.1.

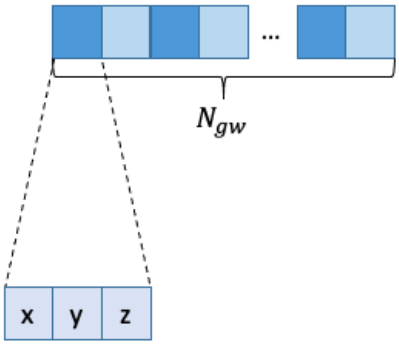

Figure 4.1: Chromosome employed for the optimization LoRaWAN smart metering network.

The chromosome represents the GW positions. In this part, each gene represents the three geographical coordinates of a GW. Since the number of gateways N_{gw} is variable, the length of this part is not constant and may vary from individual to individual.

4.1.3 Crossover

The crossover performs the exchange of genetic material between two individuals. The number of crossover operations performed in each iteration is calculated as follows:

$$n_{cross} = N_{pop}.p_{cross}, \tag{4.1}$$

where N_{pop} is the size of the population and p_{cross} is the crossover probability. The adopted crossover operator is a modification of the operator implemented in [18], and is depicted in Figure 4.2 .

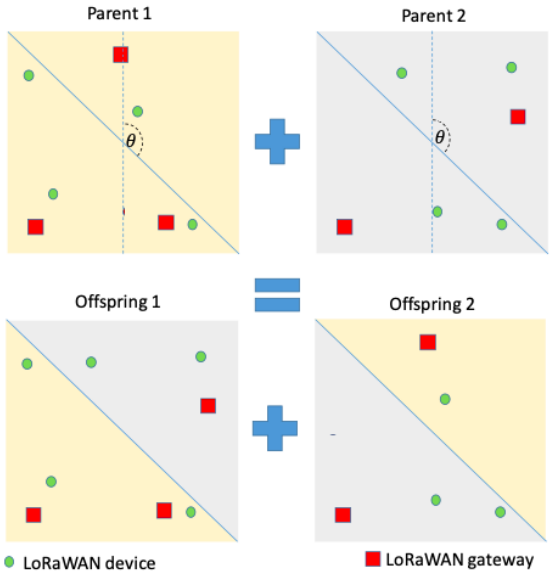

Figure 4.2: Crossover operator.

The geographical area is divided in two halves based on a random angle $\theta \in [0, \pi]$. The GWs and respective locations of one half of a parent individual is concatenated with the GWs of the opposite half of the other parent individual. In this way, two offspring individuals are generated.

4.1.4 Mutation

The mutation operator aims at genetic diversity by performing random changes to existing individuals in the population. In each iteration, a number n_{mut} of population individuals is mutated. This number is computed in the following way:

$$n_{mut} = p_{mut}.N_{pop}, \tag{4.2}$$

where p_{mut} is the mutation probability. The possible mutations that can take place in selected individuals are the following:

- Adding a gateway in a random position (probability p_{add}).
- Removing a randomly chosen gateway (probability p_{rem}).
- Randomly displacing a gateway within an are corresponding to a fraction $\sum_{mut}$ of the horizontal and vertical dimensions of the scenario (probability p_{dis}).

The first three operations exclude each other, so that only one of them is chosen randomly. We have that p_{add}+p_{rem}+p_{dis}=1.

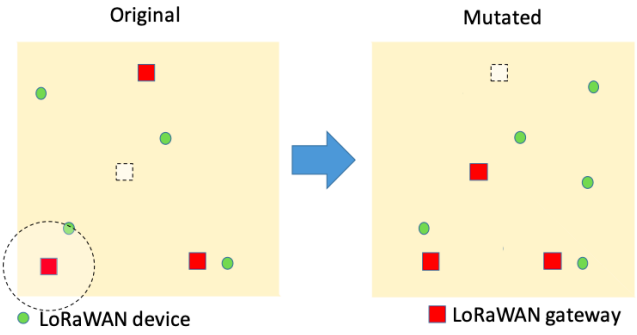

Figure 4.3: Mutation operations.

The mutation operations are depicted in Figure 4.3, where all of them appear simultaneously. In the implemented algorithm, only one of the GW operations can be performed in a single iteration.

Chapter 5

Performance Evaluation

In this Chapter, the results obtained from simulations of LoRaWAN network performance using different propagation models are presented. Numerical results obtained with the modeling methodology are discussed for different simulations.

5.1 Simulation Results

The NSGA-II implementation was run in a scenario with 500 devices randomly deployed in a circle of radius 14724 m. This deployment was developed for all propagation models: log-distance path loss, fading, shadowing and fading plus shadowing propagation model.

An example of this devices deployment is depicted in Figure 5.1. The devices are represented in colors according to their SF assignment. The green color represents the devices with the lowest SF and the red color represents the ones with the highest. Devices that weren't assigned with a SF value are represented with a black color.

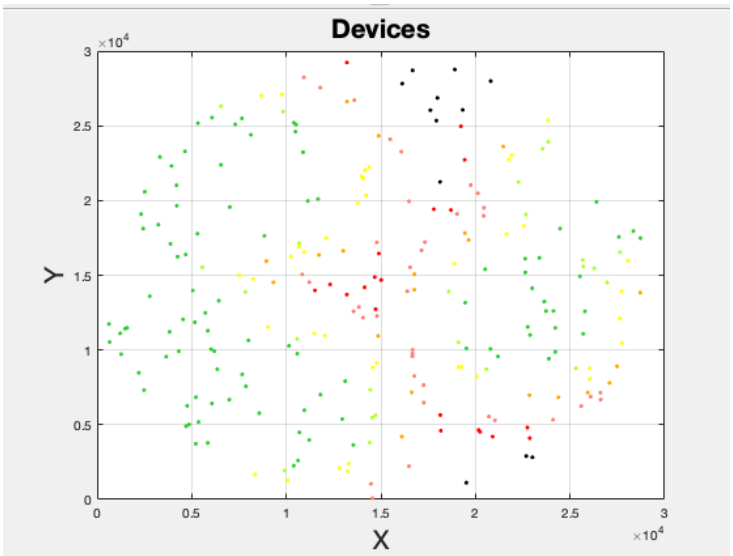

Figure 5.1: 500 Device deployment positions.

To simulate the LoRaWAN network with all the propagation models and explanations provided in previous sections, the following tables show the values chosen for the simulations. Table 5.1 shows which model distribution was used for each propagation effect and Table 5.2 lists the receiver sensitivities for the devices and GWs, for each SF.

Table 5.1: Propagation model

Path loss model	Log-distance
Fading model	Rayleigh
Shadowing model	Log-Normal
σ	3.5 dB
Interference model	ALOHA collision probability + SIR matrix

Table 5.2: Devices and Gateways receiver Sensitivities

Devices Sensistivity	SF7:-127.0 SF8: -129.5 SF9: -132.0 SF10: -134.5 SF11: -137.0 SF12: -139.5
Gateway Receiver Sensitivity	SF7 : -130.0 SF8:-132.5 SF9:-135.0 SF10:-137.5 SF11:-140.0 SF12: -142.5

The LoRaWAN parameters and NSGA-II parameters used for the simulations in Section 5.2 are listed in Tables 5.3 and 5.4.

Table 5.3: LoRaWAN parameters

Simulation scenario	Circle of radius 7362 m
Transmission power	14 dBm
Frequency	868 MHz
Bandwidth	125 KHz
d_0	1m
PL_0	8.1 dB
path loss exponent n	3.76
Code rate	4
Packey payload length	20 Bytes
overload	13 Bytes
nº bits preamble	8 bits
Packet arrival rate of each device	0.0017 packets/s
LoRaWAN sub-bands	G (3 channels)
Spreading factor	[7:12]

Table 5.4: NSGA-II parameters

Minimum number of gateways	1
Maximum number of gateways	10
Population size N_{pop}	500
Crossover percentage p_{cross}	0.7
Mutation percentage p_{mut}	0.4
Mutation rate mu	0.06
Mutation Step Size fraction	0.5
Stopping criteria	$>$ 10 iterations with same population
Fading and Shadowing channel instances	5

5.2 Simulation Results with different propagation model

In this Chapter, the results obtained from simulations of LoRaWAN network performance using different propagation models are presented.

5.2.1 Simulation Results with Log-distance propagation model

By analyzing Figure 5.2, the trade-off can be clearly distinguished, as an increase in capacity corresponds to an increase in the number of GWs of the solution, and vice-versa. Also, it is explicit that there is a performance improvement of the algorithm solutions from the initial population to the final population. The initial population hasn't as much solutions for the number of GWs as the final population.

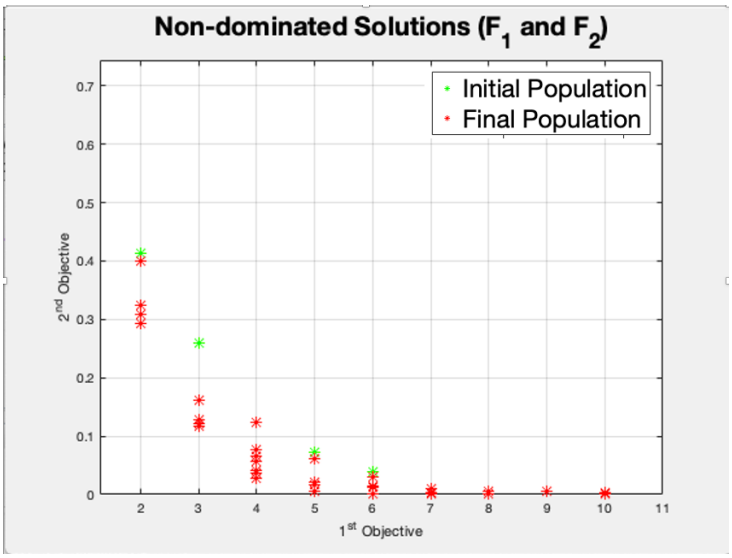

Figure 5.2: Log-distance propagation model: Initial Population Vs Population at Stopping criteria.

5.2.2 Simulation Results with Fading model

The results of this simulation represented in Figure 5.3 show that, for the same number of GWs, the packet loss decreases compared to the log-distance propagation model.

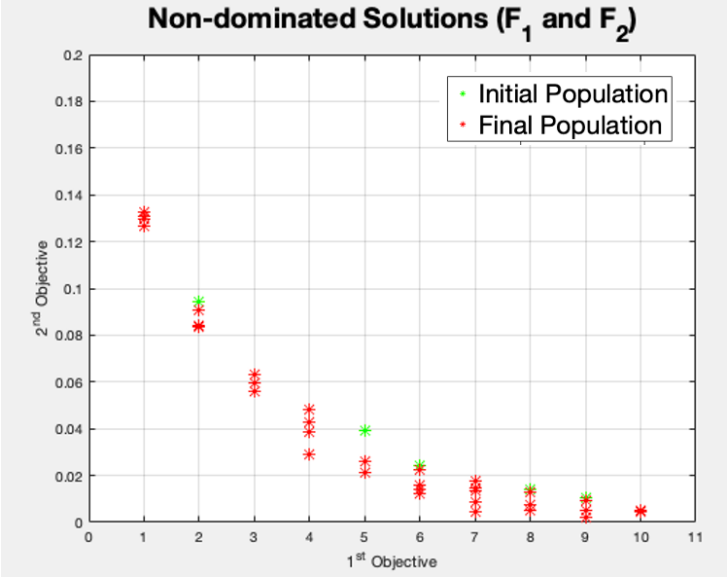

Figure 5.3: Fading propagation model: Initial population Vs Population at Stopping Criteria.

5.2.3 Simulation Results with Shadowing model

In these simulations, we can notice that the shadowing effect also reduces the interference of the signal propagation similar to the fading effect. However, in this case, the decrease of the packet loss is even more significant.

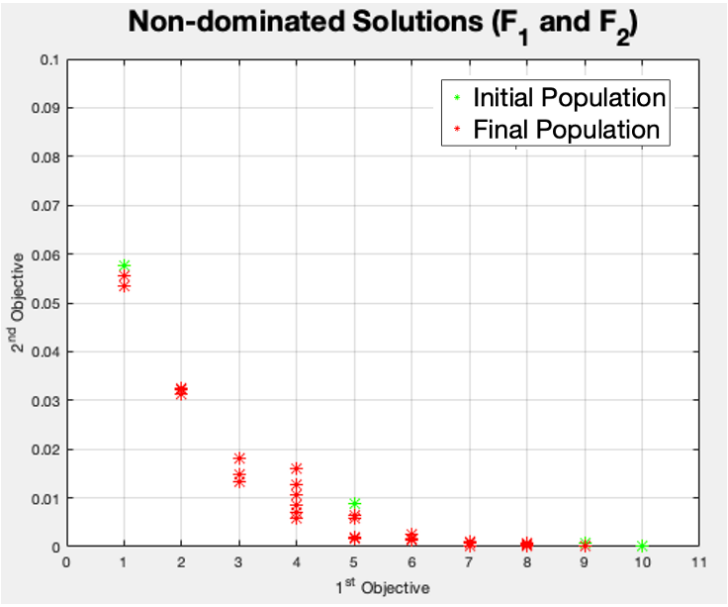

Figure 5.4: Shadowing propagation model: Initial population Vs Population at Stopping Criteria.

5.2.4 Simulation Results with Fading and Shadowing model

Taking into account the observations presented in the previous simulations, in Section 5.2.2 and Section 5.2.3 the same conclusion is to be expected in this propagation model.

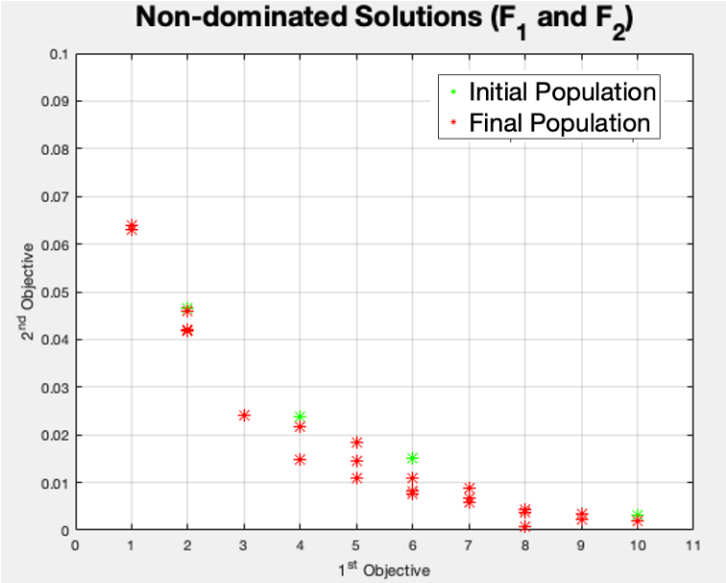

Figure 5.5: Shadowing and Fading propagation model: Initial population Vs Population at Stopping Criteria.

Therefore, it seems that the fading or shadowing effect tends to significantly reduce instantaneous interference and this effect has more impact than the effect on the main signal power, with the overall effect of reducing the packet loss ratio, which could be assumed to be counter-intuitive.

In an effort of explaining this performance, numerical results were obtained for the average PLR as a function of the number of devices in a scenario in which the devices are randomly deployed within a circle of radius 7362 m around a single GW. In Figures 5.6, 5.7, 5.8 and 5.9 the device's SF assignment in the different propagation models scenarios, and with one GW in the center are represented .

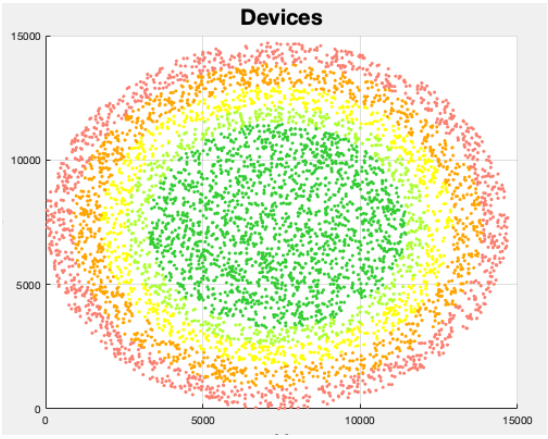

Figure 5.6: SFs with no attenuation effects

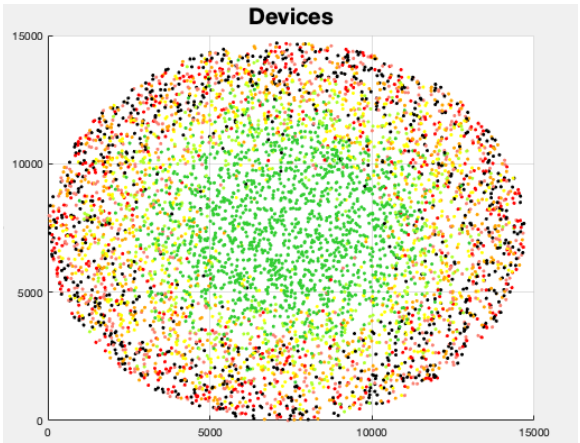

Figure 5.7: SFs with fading

As mentioned in Section 5.2.4, the fading or shadowing effect tends to reduce instantaneous interference as well as the packet loss ratio. This result is unpredictable at first since it would be presumed that

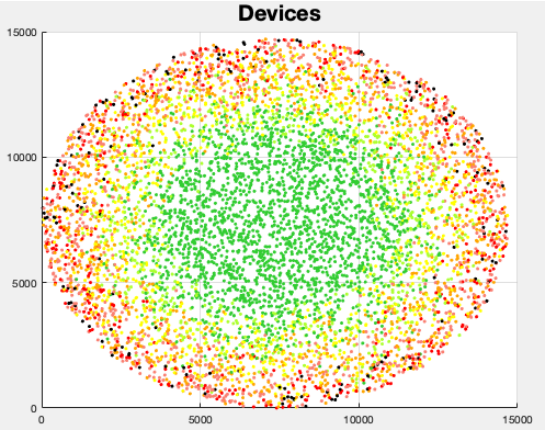

Figure 5.8: SFs with shadowing

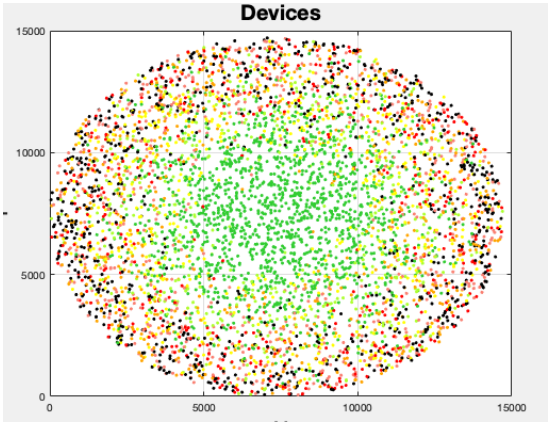

Figure 5.9: SFs with shadowing and fading

these events would increase both interference and the packet loss ratio.

However, since the simulation area has a small radius and this study's SF allocation procedure is distance-dependent it may happen the decrease of collision probability in the presence of fading or shadowing.

In fact, because of fading, spreading factors are randomly distributed over the simulated area, which reduces Co-SF interference in small cells. This result is also related to the way SFs are assigned in the current model, which chooses the lowest SF possible for the expected received power.

As illustrated in Figure 5.6, the SF are uniformly distributed in the case of Log-distance propagation model. However, in the other model cases, with fading or shadowing effect, the distribution is not uniform. This means that different values of the SFs, will consequently lead to a decrease in collisions. Orthogonal SFs enables simultaneous transmissions at different data rates on the same frequency channel.

Chapter 6

Conclusions

In this Chapter, some conclusions about this Master Thesis are drawn, specifying the achievements of this work, interpreting the obtained results and discussing some future possible improvements for this work.

6.1 Achievements

The major purpose of this Master Thesis was to implement a LoraWAN network analytical model and optimize the GWs positions using NSGA-II as well as study the impact of fading and shadowing on the network's deployment.

The challenges of the quality of the signal reception led to the development of different propagation models to study the network's deployment.

This master thesis executed a LoRaWAN analytical model developed by INESC in the WiMeCOM project [13]. The first contributions are proposed with the study of fading and shadowing in the quality performance of the network. Results show that the fading or shadowing effect leads to the decrease of instantaneous interference as well as the packet loss ratio. This has a significant impact on the GW placement. This effect was validated and considered to be related to the orthogonality of the SFs assigned to the devices, which leads to a decrease of collisions. This result is also related to the way SFs are assigned in the current model, which chooses the lowest SF possible for the expected received power.

It must be highlighted that this performance may have different results in other simulation environments. In this study, we consider that transmissions that reach a GW are independent from those that reach neighbor GWs. However, in real scenarios, the transmission from a node will likely reach more than one gateway, creating inter-dependency between packet vulnerable times. While the inability to consider this statistical dependency reduces the complexity of the WiMeCOM model, it may have a significant impact on the obtained results. Furthermore, the current model assumes static SF assignment, which is adequate for a log-distance model, but not for a model that integrates fading effects. In a true scenario, the Adaptive Data Rate mechanism of LoRaWAN would respond to changes in the signal power, changing the SF used by each device. However, such dynamic mechanisms are difficult to model analytically,

where worst-case or average conditions are usually assumed. Discrete event simulation should be used to find the correct parameters and correct the analytical model.

6.2 Future Work

This master thesis has some directions for future work. Firstly, this study should be developed for a 5G network and analyze if there are the same observations for the effect of fading and shadowing in this type of network.

Additionally, the interference between gateways should be taken into account as this study is considering each GW as an isolated device.

Adaptive optimization of the SFs should also be considered to ensure more realistic results. This development can consume time but the simulations would be more reliable.

Implement Machine Learning techniques to give more immediate answers. For example, use a neural network, that could be trained with the results of the NSGA-II and provide new configurations for the GWs.

Bibliography

[1] M. de Castro Tomé, P. H. Nardelli, and H. Alves. Long-range low-power wireless networks and sampling strategies in electricity metering. *IEEE Transactions on Industrial Electronics*, 66(2): 1629–1637, 2018.

[2] L. Alliance. *A technical overview of LoRa and LoRaWAN*. 2015. URL `https://lora-alliance.org/sites/default/files/2018-04/what-is-lorawan.pdf`.

[3] K. Mekki, E. Bajic, F. Chaxel, and F. Meyer. A comparative study of lpwan technologies for large-scale iot deployment. *ICT express*, 5(1):1–7, 2019.

[4] H. Mroue, A. Nasser, B. Parrein, S. Hamrioui, E. Mona-Cruz, and G. Rouyer. Analytical and simulation study for lora modulation. In *2018 25th International Conference on Telecommunications (ICT)*, pages 655–659. IEEE, 2018.

[5] L. Alliance. Lorawan™ 1.0. 2 regional parameters. *no. Feb*, pages 1–55, 2017.

[6] D. Bankov, E. Khorov, and A. Lyakhov. On the limits of lorawan channel access. In *2016 International Conference on Engineering and Telecommunication (EnT)*, pages 10–14. IEEE, 2016.

[7] N. Sornin, M. Luis, T. Eirich, T. Kramp, and O. Hersent. Lorawan specification. *LoRa alliance*, 2015.

[8] P. Ngatchou, A. Zarei, and A. El-Sharkawi. Pareto multi objective optimization. In *Proceedings of the 13th International Conference on, Intelligent Systems Application to Power Systems*, pages 84–91. IEEE, 2005.

[9] V. L. Vachhani, V. K. Dabhi, and H. B. Prajapati. Survey of multi objective evolutionary algorithms. In *2015 International Conference on Circuits, Power and Computing Technologies [ICCPCT-2015]*, pages 1–9. IEEE, 2015.

[10] K. Deb, A. Pratap, S. Agarwal, and T. Meyarivan. A fast and elitist multiobjective genetic algorithm: Nsga-ii. *IEEE transactions on evolutionary computation*, 6(2):182–197, 2002.

[11] M. Garau, G. Celli, E. Ghiani, F. Pilo, and S. Corti. Evaluation of smart grid communication technologies with a co-simulation platform. *IEEE Wireless Communications*, 24(2):42–49, 2017.

[12] D. Magrin, M. Centenaro, and L. Vangelista. Performance evaluation of lora networks in a smart city scenario. In *2017 IEEE International Conference on Communications (ICC)*, pages 1–7. ieee, 2017.

[13] A. M. R. C. Grilo. A moroccan wireless smart metering solution (wimecom). 2019.

[14] R. W. Heath Jr. *Introduction to Wireless Digital Communication: A Signal Processing Perspective*. Prentice Hall, 2017.

[15] J. Miranda, R. Abrishambaf, T. Gomes, P. Gonçalves, J. Cabral, A. Tavares, and J. Monteiro. Path loss exponent analysis in wireless sensor networks: Experimental evaluation. In *2013 11th IEEE international conference on industrial informatics (INDIN)*, pages 54–58. IEEE, 2013.

[16] R. B. Sørensen, D. M. Kim, J. J. Nielsen, and P. Popovski. Analysis of latency and mac-layer performance for class a lorawan. *IEEE Wireless Communications Letters*, 6(5):566–569, 2017.

[17] B. H. Liu, B. P. Otis, S. Challa, P. Axon, C. Chou, and S. Jha. The impact of fading and shadowing on the network performance of wireless sensor networks. *International Journal of Sensor Networks*, 3(4):211–223, 2008.

[18] S. Sabino, N. Horta, and A. Grilo. Centralized unmanned aerial vehicle mesh network placement scheme: A multi-objective evolutionary algorithm approach. *Sensors*, 18(12):4387, 2018.

.